Åbo Akademi University

Jerzy Jasielec

Modelling of Potentiometric Ion Sensors

Modelling of Potentiometric Ion Sensors

Jerzy Jasielec

Laboratory of Analytical Chemistry
Process Chemistry Center
Department of Chemical Engineering
Åbo Akademi University
Åbo/Turku, Finland
2013

Supervised by

Docent Tomasz Sokalski
Laboratory of Analytical Chemistry
Åbo Akademi University
Åbo, Finland

Professor Andrzej Lewenstam
Laboratory of Analytical Chemistry
Åbo Akademi University
Åbo, Finland

Department of Materials Science and Ceramics
AGH – University of Science and Technology
Kraków, Poland

Reviewer and Opponent

Professor Richard Compton
Department of Chemistry
Oxford University
Oxford, UK

Reviewer

Professor Władysław Kubiak
Department of Materials Science and Ceramics
AGH – University of Science and Technology
Kraków, Poland

ISBN 978-952-12-2938-1
Painosalama Oy – Turku, Finland 2013

"All truths are easy to understand once they are discovered;
the point is to discover them."
Galileo Galilei

To My Dear Friends and Family

Table of Contents

Preface

The research work presented in this thesis was mainly carried out in the Laboratory of Analytical Chemistry at Åbo Akademi University as a part of activities of the Åbo Akademi Process Chemistry Centre. Funding from the Graduate School of Chemical Engineering (GSCE) and the Rector of Åbo Akademi is gratefully acknowledged.

I have been very lucky to come across and work with many wonderful people during my last research years. These years were an interesting and chastening journey, introducing me to a variety of projects and the world of scientific knowledge, giving me many joyful moments. For these happy moments, I would like to give my special thanks to a numerous people who have influenced my personal development.

First of all, I would like to thank my Mentors, Docent Tomasz Sokalski and Professor Andrzej Lewenstam. Under their supervision I grew up from a simple student to a researcher. Thank you for your trust in me, time, encouragement, guidance, tireless advice, involvement in my scientific development and patience throughout the work. I would also like to thank Professor Ari Ivaska for his positive and helpful attitude towards my scientific activity, introducing me to the Graduate School of Chemical Engineering and treating me kindly throughout this scientific journey. Many thanks!

This work would not be possible without the involvement of many people. I would like to thank Professor Marek Danielewski and Dr hab. Robert Filipek from AGH - University of Science and Technology, for welcoming me in their group and collaborating in joint projects. I would also like to thank their group: Dr Bartłomiej Wierzba, Dr Krzysztof Szyszkiewicz and Dr Bartosz Grysakowski. It was a pleasure to work with you.

I had a such a wonderful time working in the Laboratory of Analytical Chemistry at Åbo Akademi and wish to express my thanks to the head of our laboratory, Professor Johan Bobacka, as well as to my wonderful present and former colleagues: Dr Grzegorz Lisak, Michał Wagner, Ulrika Vanamo, TingTing Han, Dr Zekra Mousavi, Kim Granholm, Victoria Mäkimartti, Docent Tom Lindfors, Anna and Lotta Österholm, Dr Marceline Neg Akieh-Pirkanniemi, Dr Gordon Driver, Dr Maija Blomquist, Dr Fredrik Sundfors, and Professor Kalle Levon. You have made my work in this Laboratory very enjoyable.

I would like to thank the Graduate School in Chemical Engineering, not only for the financial support, but also for giving me opportunity to meet many fellow researchers all over Finland. Special thanks to Maria Ljung for her forbearance and help with formal issues.

The past years wouldn't be the same without my involvement in the activities of the Erasmus Student Network. I would like to thank all my friends around the world who have always given me valued support in this voluntary work. Firstly, thanks to members of the ESN Network and Events Committee, whom I had the pleasure to lead during the last year: Emre Emirioglu, Katja Krohn, Vincent Janiak, Asia Maziarz, Michaela Zormanova, Jiri Andrejs, Elisa Priolo, Tomas Sandberg and others. Secondly, thanks to my dear friends involved in the actions of ESN International, among them: Simona Patasiute, Carmen Cuesta Roca, Stefan Jahnke, Salih Odobasi, Damien Lamy-Preto, Juan Colino, Fabian Bircher, Prokop Teper, Lora Zasheva, Giulia Rosa D'Amico, Giovanni Giaccobi, Madara Apsalone and Kadir Keles. Also, thanks to the present and former members of my home section, ESN vid Åbo Akademi: Oscar Boije, Timo Schmidt, Aino Lyytikainen, Mohammad Bagher Khajeheian, Joel Nyström, Maria Helenius and others. Thank you all for sharing many amazing experiences with me, your help and advice. Thank you. Tack. Danke. Ви благодариме. Merci. Dzięki. Děkuji. Grazie. Kiitos. Ačiū. Teşekkürler. Gracias. Благодаря. Paldies.

Special thanks to my good friends in Finland, Christian Sergelius and Markus Kankonnen. Without you, my stay in Finland wouldn't be as interesting as it was. Thanks to my life-long friends in Poland: Bartłomiej and Katarzyna Lis, as well as Jakub and Grzegorz Domagała. Thank you all for your support, cheerfulness, help when I needed it, and all the moments we spent together.

Last, but not least, I owe my deepest gratitude to my loving family. Special thanks to my parents Anna and Janusz, sister Katarzyna and grandparents Danuta and Adam for your eternal support, encouragement, and belief in my success. All I achieved I own to you. Dziękuję Wam z całego serca!

Abstract

Potentiometric ion sensors are a very important subgroup of electrochemical sensors, very attractive for practical applications due to their small size, portability, low-energy consumption, relatively low cost and not changing the sample composition. They are investigated by the researchers from many fields of science. The continuous development of this field creates the necessity for a detailed description of sensor response and the electrochemical processes important in the practical applications of ion sensors.

The aim of this thesis is to present the existing models available for the description of potentiometric ion sensors as well as their applicability and limitations. This includes the description of the diffusion potential occurring at the reference electrodes. The wide range of existing models, from most idealised phase boundary models to most general models, including migration, is discussed. This work concentrates on the advanced modelling of ion sensors, namely the Nernst-Planck-Poisson (NPP) model, which is the most general of the presented models, therefore the most widely applicable. It allows the modelling of the transport processes occurring in ion sensors and generating the potentiometric response.

Details of the solution of the NPP model (including the numerical methods used) are shown. The comparisons between NPP and the more idealized models are presented. The applicability of the model to describe the formation of diffusion potential in reference electrode, the lower detection limit of both ion-exchanger and neutral carrier electrodes and the effect of the complexation in the membrane are discussed. The model was applied for the description of both types of electrodes, i.e. with the inner filling solution and solid-contact electrodes.

The NPP model allows the electrochemical methods other than potentiometry to be described. Application of this model in Electrochemical Impedance Spectroscopy is discussed and a possible use in chrono-potentiometry is indicated.

By combining the NPP model with evolutionary algorithms, namely Hierarchical Genetic Strategy (HGS), a novel method allowing the facilitation of the design of ion sensors was created. It is described in detail in this thesis and its possible applications in the field of ion sensors are indicated.

Finally, some interesting effects occurring in the ion sensors (i.e. overshot response and influence of anionic sites) as well as the possible applications of NPP in biochemistry are described.

Referat

Potentiometriska jonsensorer är en mycket viktig undergrupp av elektrokemiska sensorer. De är mycket attraktiva i praktiska tillämpningar på grund av sina ringa storlekar, portabilitet, låga energiförbrukning, relativt låga kostnad och de förändrar inte provets sammansättning. De undersöks av forskare från många vetenskapsområden. Den kontinuerliga utvecklingen av detta forskningsområde skapar ett behov av en detaljerad beskrivning av sensorernas respons och de elektrokemiska processerna som är viktigt i praktiska tillämpningar av jonsensorer.

Syftet med denna avhandling är att presentera existerande modeller för att beskriva potentiometriska jonsensorer samt deras användbarhet och begränsningar. Detta inkluderar en beskrivning av diffusionspotentialen som inträffar vid referenselektroder. Det breda utbudet av befintliga modeller, allt ifrån de mest idealiserade fasgränsmodeller till de mest generella modeller inklusive migrationen, diskuteras. Detta arbete koncentrerar sig på avancerad modellering av jonsensorer, nämligen Nernst-Planck-Poisson (NPP) modellen, vilken är den mest generella av de presenterade modellerna och är därför även den mest tillämpbara. Den tillåter modellering av transportprocesser som förekommer i jonsensorer och genererar det potentiometriska responsen.

Detaljer från lösningen av NPP-modellen (inkluderat de använda numeriska metoderna) visas. Jämförelser mellan NPP och mer idealiserade modeller presenteras. Tillämpligheten av modellen, för att beskriva bildandet av diffusionspotentialen i referenselektroden, den låga detektionsgränsen för både jonbytare och neutrala elektrodbärare samt effekten av komplexbildning i membranet, diskuteras. Modellen var tillämpad för att beskriva både elektroder med inre lösning och elektroder med fast-kontakt.

NPP-modellen tillåter även beskrivning av andra elektrokemiska metoder än potentiometri. Tillämpning av denna modell i elektrokemisk impedansspektroskopi diskuteras och en eventuell användning i chrono-potentiometri indikeras.

Genom att kombinera NPP-modellen med evolutionära algoritmer, nämligen Hierarchichal Genetisk Strategi (HGS), skapades en ny metod som gör det möjligt att förenkla designen av jonsensorer. Det beskrivs i detalj i denna avhandling och dess möjliga tillämpningar inom området för jonsensorer anges.

Slutligen beskrivs några intressanta effekter som uppträder i dessa jonsensorer (dvs. överskjuten signal och inflytande av anjoniska säten) och möjliga tillämpningar av NPP inom biokemi.

List of publications

This thesis is based on the following publications, which are referred to in the text by their Roman numerals. The included original publications are re-printed with the permission of the copyright holders.

I. J.J. Jasielec, T. Sokalski, R. Filipek, A. Lewenstam; ***Comparison of different approaches to the description of the detection limit of ion-selective electrodes***; Electrochimica Acta 55 (2010), 6836-6848.

II. J.J. Jasielec, B. Wierzba, B. Grysakowski, T. Sokalski, M. Danielewski, A. Lewenstam; ***Novel Strategy for Finding the Optimal Parameters of Ion Selective Electrodes***; ECS Trans. 33 (26), 19 (2011), 19-29.

III. J.J. Jasielec, K.Szyszkiewicz, R. Filipek, J. Fausek, M. Danielewski, A. Lewenstam; ***Computer simulations of Electrodiffusion Problems Based on Nernst-Planck and Poisson Equations***; Computational Materials Science 63 (2012), 75–90.

IV. J.J. Jasielec, G. Lisak, M. Wagner, T. Sokalski, A. Lewenstam; ***Nernst-Planck-Poisson Model for the Qualitative Description of the Behaviour of Solid-Contact Ion-Selective-Electrodes at Low Analyte Concentration***; Electroanalysis 25 (2013), 133 – 140.

V. A. Lewenstam, T. Sokalski, J. Jasielec, W. Kucza, R. Filipek, B. Wierzba, M. Danielewski; ***Modelling Non Equilibrium Potentiometry to Understand and Control Selectivity and Detection Limit;*** ECS Transactions 2009, 19, 219-224.

VI. B. Grysakowski, J.J. Jasielec, B. Wierzba, T. Sokalski, A. Lewenstam and M. Danielewski; ***Electrochemical Impedance Spectroscopy (EIS) of Ion Sensors. Direct modelling and inverse problem solving using the Nernst-Planck-Poisson (NPP) model and the HGS(FP) optimization strategy;*** J. Electroanal. Chem. 662 (2011), 143-149.

Contribution of the author:

Publication I – The author wrote the computer program used for numerical simulations, performed the numerical simulations, wrote the first draft of the manuscript, and finalized it in collaboration with the co-authors.

Publication II – The author wrote the computer program used for numerical simulations together with one of the co-authors, performed the numerical simulations, wrote the first draft of the manuscript, and finalized it in collaboration with the co-authors.

Publication III – The author wrote the computer program used for numerical simulations, performed the numerical simulations together with other co-authors, wrote the first draft

of the manuscript together with other co-authors, and finalized it in collaboration with the co-authors.

Publication IV – The author wrote the computer program used for numerical simulations, performed the numerical simulations, compared the numerical results with the experimental results obtained by one of the co-authors, wrote the first draft of the manuscript, and finalized it in collaboration with the co-authors.

Publication V – The author finalized the manuscript in collaboration with the co-authors.

Publication VI – The author wrote the computer program used for numerical simulations for method using Heavy-side function excitation, performed some of the numerical simulations, wrote the first draft of the manuscript together with co-authors, and finalized it in collaboration with the co-authors.

Abbreviations and symbols

A – electrode surface
Ag – Silver
a_i – activity of the *i*-th ion
a_i^j – rescaling constant
b_i^j – rescaling constant
$c_{i,L}$ – concentration of the *i*-th ion in the bulk of sample solution (left side of the system)
$c_{i,R}$ – concentration of the *i*-th ion in the inner solution (right side of the system)
c_i^j – concentration of the *i*-th ion in the *j*-th phase
$\bar{c}_i^j$ – dimensionless (rescaled) concentration of the *i*-th ion in the *j*-th phase
c_{mixt}^j – average molar concentration of in the *j*-th phase
$c_i^{j,k}$ – concentration of the *i*-th ion in the *k*-th discreet point of the *j*-th layer
c_i^M – concentration of the *i*-th ion in the membrane phase
$c_{i0}^M(t)$ – concentrations of the *i*-th ion in the membrane at the interface membrane | solution at time *t*
c_i^S – concentration of the *i*-th ion in the bulk of sample solution
$c_{i0}^S(t)$ – concentrations of the *i*-th ion in the sample solution at the interface membrane | solution at time *t*
c_s – concentration characteristic constant (scaling factor)
Ca^{2+} – calcium ion
Cl – Chlorine
CP – conducting polymer
CWE – coated-wire electrode
d_j – width of the *j*-th layer (phase)
D_i – diffusion coefficient of the *i*-th ion
D_i^j – diffusion coefficient of the *i*-th ion in the *j*-th layer (phase)
DLM – Diffusion Layer Model
DP – diffusion parameter (in SDM)
E^j – electric field in the *j*-th layer
$\bar{E}^j$ – dimensionless (rescaled) electric field in the *j*-th layer
$E^{j,k}$ – electric field in the *k*-th descreet point in the *j*-th layer
E_s – electric field characteristic constant (scaling factor)
EbT – Eriochrome Black T
EIS – Electrochemical Impedance Spectroscopy
ESGA – Elitist Simple Genetic Algorithm
F – Faraday constant
f_l – vector of *l* elements solved by numerical integrator
FEM – Finite Elements Method
$fitness$ – value of the fitness function (in HGS)
g^j – weight function

g_l^j – rescaling constant

Ge – Germanium

$h_{j,k}$ – distance separating *(k-1)*-th and *k*-th discreet space point in *j*-th layer

h^j – weight function

H^+ – hydrogen ion

HGS – Hierarchical Genetic Strategy

HGS-FP – Hierarchical Genetic Strategy with real number (floating point) encoding

$I(t)$ – current density

$\overline{I^j}$ – dimensionless (rescaled) current density in *j*-th layer

I^+ – preferred ion

IL^+ – complex of the preferred ion

ISE – ion-selective electrode

IUPAC – International Union of Pure and Applied Chemistry

I-ESGA – Improved Elitist Simple Genetic Algorithm

I-SGA – Improved Simple Genetic Algorithm

J_i – flux of the *i*-th ion

J_i^j – flux of the *i*-th ion in the *j*-th layer (phase)

J^+ – discriminated ion

JL^+ – complex of the discriminated ion

k_i – ion-partition constant

$k_{i,as}$ – association rate constant (for complexing the *i-th* ion)

$k_{i,dis}$ – dissociation rate constant (for complexing the *i-th* ion)

$\overrightarrow{k_{i\lambda_j}}$ – heterogeneous rate constant, which corresponds to the ion *i* moving from layer α_j to α_{j+1}

$\overrightarrow{\overline{k_{i\lambda_j}}}$ – dimensionless (rescaled) heterogeneous rate constant $\overrightarrow{k_{i\lambda_j}}$

$\overleftarrow{k_{i\lambda_j}}$ – heterogeneous rate constant, which corresponds to the ion *i* moving from layer α_{j+1} to α_j.

$\overleftarrow{\overline{k_{i\lambda_j}}}$ – dimensionless (rescaled) heterogeneous rate constant $\overrightarrow{k_{i\lambda_j}}$

K^+ – potassium ion

K_{coex} – coextraction constant

K_{exch} – exchange constant

K_{IJ} – equilibrium constant (for the reaction)

K_{IJ}^{pot} – selectivity

L – lower detection limit

LSODI – software package including Gear's integrator

Mg^{2+} – magnesium ion

MoL – Method of Lines

n – number of layers (phases)

n_{tot} – total number of sites on the membranes surface occupied by the ions

N_j – number of grid points in the *j*-th layer (phase)

Na^+ – sodium ion

NO_3^- – nitrate ion

NE – Nikolsky-Eisenman (equation)

NPP – Nernst-Planck-Poisson (model)

NPP-HGS – method combining Nernst-Planck-Poisson model and Hierarchical Genetic Strategy

ODE – ordinary differential equation

pH – *potentia hydrogenii* (logarithm of the hydrogen ion activity)

Pb^{2+} – lead ion

PBM – phase boundary model

PDE – partial differential equation

PVC – Polyvinyl chloride

r – number of components

R – gas constant

R^- and R^+ – negatively and positively charged anionic site ion

R_T – total concentration of the anionic sites

$s(t)$ – surface coverage (or site filling) factor at time t

s_{eq} – surface coverage (or site filling) factor at equilibrium

s_1 – slope of the calibration curve performed for the preferred ion

SDM – Steady State Diffusion Model

SGA – Simple Genetic Algorithm

Si – Silicon

t – time of the process

$\overline{t}$ – dimensionless (rescaled) time of the process

t_{END} – end time of the process

t_s – time characteristic constant (scaling factor)

T – absolute temperature

$TDDA^+$ – tetradodecyloamonium ion

TDM-E – time-dependent exchange model

TDM-EC – time-dependent exchange-coextraction model

$TFPB^-$ – tetrakis(4-fluorophenyl)-borate ion

$TClPB^-$ – tetrakis(4-chlorophenyl)borate ion

u_i – mobility of the i-th ion

x – space

$\overline{x}$ – dimensionless (rescaled) space

$x_{j,k}$ – k-th discreet space point in j-th layer

x_s – space characteristic constant (scaling factor)

X^- – counter-ion

X^{2+} – various bivalent impurities

$y_{j,k}$ – discreet space point placed in the middle of an interval $\left[x_{j,k-1}, x_{j,k}\right]$

z_i – charge of i-th ion

Z_{calc}^j – calculated value of complex electrochemical impedance at j-th frequency

Z_{ref}^j – reference value of complex electrochemical impedance at j-th frequency

α_j – the *j-th* layer (phase)

β_i – stability constant for the complex of *i*-th ion

δ^j – distance between two neighbouring grid points

$\Delta\varphi$ – overall potential in the system

ε_j – dielectric permittivity in the *j*-th layer

ε_{av} – average dielectric permittivity

λ_j – right-side boundary of the *j*-th phase (also left-side boundary of the *(j+1)*-th phase)

φ – electrical potential

φ_D – diffusion potential

φ_I – electrical potential for the calibration in the preferred ion

φ_J – electrical potential for the calibration in the discriminated ion

φ_M – equilibrium potential

φ_{PB} – phase boundary potential

φ_L – electrical potential at the left side of the membrane

φ_R – electrical potential at the right side of the membrane

φ^j – electrical potential in the *j*-th layer

$\varphi^{j,k}$ – electrical potential in the *k*-th discreet point in the *j*-th layer

$\tilde{\mu}_i$ – electrochemical potential of the *i*-th ion

μ_i – chemical potential of the *i*-th ion

μ_i^0 – chemical potential of the *i*-th ion under standard conditions

υ^j – drift velocity (in the *j*-th layer)

1. Introduction

Potentiometric ion sensors, namely ion-selective electrodes (ISEs) and ion-sensitive sensors are a very important subgroup of electrochemical sensors [1]. They allow potentiometric determination of the activity of certain ion in the presence of other ions. They are very attractive for practical applications due to their features, such as small size, portability, low-energy consumption, and relatively low cost.

Many scientists are continuously and intensively searching for novel electrode materials and new constructions, as well as the new applications for ion sensors. The field of ion sensors is an example of multidisciplinary research in chemistry, conducted by physiologists, physicochemists, electrochemists, analytical chemists, membrane experts, extraction specialists, and researchers interested in practical applications and manufacturing the electrodes [2]. Instrumentation and sensors in potentiometric measurements are relatively cheaper and more user-friendly than in other analytical techniques. Furthermore, the measurements do not change the sample composition [3].

The typical setup for the potentiometric measurements consists of the ion-selective electrode and the external reference electrode, as shown in Fig. 1. The ion selective electrode consists of the ion-sensitive membrane, internal reference electrode and inner electrolyte solution (in case of the solid-contact electrodes, two latter may be substituted e.g. by conducting polymer deposited on a substrate).

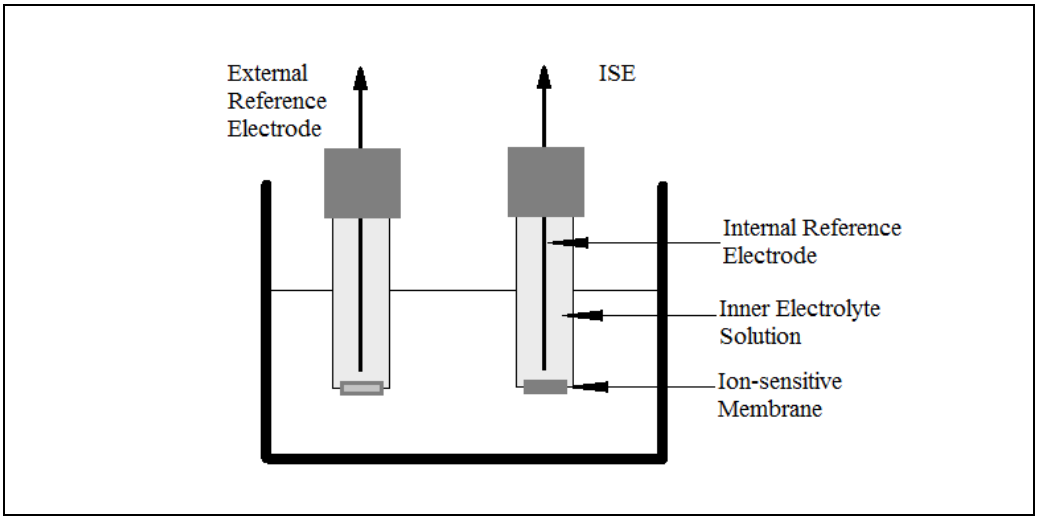

Figure 1. *The typical setup for the potentiometric measurements.*

The first ISE, a glass electrode, was invented in 1909 [2]. Since then the popularity of ISEs has increased and the research concerning the possible ion-selective materials for applications in this particular field has been continuously advancing.

The solid state membranes could serve as the ion-selective materials. The first approaches to use such membranes were presented in 1921 by Trümpler [4] and later by Kolthoff and Sanders [5], who proposed membrane materials in the form of disk casts from silver salt melts. One of the first workable electrodes based on crystalline materials was iodide-sensitive membrane, presented by Pungor and Hollós-Rokosinyi [6]. A real break-through in the field of ion-selective electrodes came with the homogeneous ion-exchanger membrane composed of a single crystal in 1966 by Frant and Ross [7]. The reviews of Pungor and Tóth [8,9,10] show the variety of applications of different crystalline materials.

The preparation of another type of ion-selective materials - polymeric membranes was pioneered in 1960's by Shatkay [11,12] and later refined by Moody and Thomas [13]. Nowadays, ISEs based on polymeric membranes are available for the determination of a large number of ions (both organic and inorganic), as it was described in the end of 1990s, in the extensive reviews [14,15].

ISEs are used in many different applications from life sciences to environmental control. Many reviews and books are dedicated to this topic. Among others, it is worth mentioning works by Purves [16], Ammann [17] and Takahashi et al. [18].

ISEs found applications in flow analysis, namely for fluidic microsystems [19], measurements in flowing solutions [20] or for the analysis by the flow-injection technique [21]. In life sciences and biology ISEs were used (among other applications) to investigate transportation of ions in plants [22], for measurements in biological tissues [23], or to study the cell volume regulation mechanism of nerve cells [24]. In environmental analysis ISEs can be used e.g. for determination of a variety of ions in water samples [25] or for studying a biological phosphorus removal process [26].

The vivid development of this field creates the necessity for a detailed description of sensors response (including its dependency on various parameters), as well as the electrochemical processes important in the practical applications of ion sensors. Most recently, the theoretical description of the ion sensors requires methods from the fields of advanced mathematics and computer science.

The aim of this thesis is to present the existing models available for the description of potentiometric ion sensors, as well as their applicability and limitations. This includes the description of the diffusion potential occurring at the reference electrodes. The wide range

of existing models from most idealised phase boundary models to most general models including migration is discussed. This work concentrates on the advanced modelling of ion sensors, namely the Nernst-Planck-Poisson (NPP) model, which is the most general of the presented models, therefore the most widely applicable. It allows the modelling of the transport processes occurring in ion sensors and generating the potentiometric response.

Details of the solution of NPP model (including the numerical methods used) are shown. The comparisons between NPP and the more idealized models are presented. The applicability of the model for both ion-exchanger and neutral carrier electrodes, as well as the formation of diffusion potential (liquid junction case), is discussed.

The NPP model allows the description of the electrochemical methods other than potentiometry. Application of this model in Electrochemical Impedance Spectroscopy is discussed and a possible use in chrono-potentiometry is also indicated.

By combining the NPP model with evolutionary algorithms, namely Hierarchical Genetic Strategy (HGS), a novel method allowing the facilitation of the design of ion sensors was created. It is described in detail in this thesis and its possible applications in the field of ion sensors are indicated.

Finally, some interesting effects occurring in the ion sensors (i.e. overshot response and influence of anionic sites), as well as the possible applications of NPP in biochemistry are described.

The issues mentioned above belong to the forefront challenges of analytical science.

2. Modelling of Sensor Response

The formation of the membrane potential of ion-selective electrodes (ISEs) is a complex, time-dependent phenomenon and depends on the thermodynamic and kinetic properties of the membrane | solution system, as well as the composition and properties of the electroactive material (membrane/film) and the bathing solution.

The first theory for the electrode potential was developed by Dole [27] and later reformulated by Nikolsky [28]. In 1960s, both Nikolsky with his group [29,30] and Eisenman [31,32] independently expressed the overall membrane potential as the sum of the *boundary* and *diffusion potentials* under steady state conditions – known today as the Nikolsky-Eisenman (NE) equation [33,34]. Since then, several models for the description of ISE potential were developed. Some of them share the assumptions and simplifications of Nikolsky and Eisenman, while others take into consideration more processes and system parameters, producing problems which are more complex mathematically. While the description of ISE is very often conducted by using empirical or semi-empirical equations, other membrane sciences often use the Nernst-Planck-Poisson system of equations as a starting point [35].

There is an ongoing and vigorous debate in the literature concerning models describing the behaviour of potentiometric sensors. There are two main schools of thought: one opts for simplicity, while the second stresses generality.

The available models can be roughly divided into three categories: Phase Boundary Models (PBMs), Diffusion Layer Models (DLMs) and models including migration. They might also be divided into time-dependent and time-independent (equilibrium and steady-state) models [3].

The debate about the merits of different models has been mostly verbal, and a critical comparison between existing models was lacking so far. In the following chapters, models used for the description of potentiometric sensors' behaviour are discussed.

Modelling in the area of ion sensors serves two roles. The first, "classical" role is to support experimentalist with very basic principles of sensor response and to support quantitative measurements by simple equations. Another, "advanced" role is to provide fundamental understanding of the sensor response by helping to map electric potential and concentration changes in space and time [3].

The classical models described in chapters 2.1. – 2.3., are more idealized in order to intentionally avoid mathematical, numerical and computational difficulties. They are easier to comprehend and to present. It is possible to reduce the more general model to a less general one, but not possible to deduce a more general model from a less general one [3]. In contrast to the classical approaches, the advanced models are the only way to achieve the fundamental understanding of a sensor response. It is because the classical models do not include the migration process, which leads to non-adequate space and time-dependent characteristic of sensor response.

In all of the discussed models, it is assumed that the potentiometric response is modelled under open-circuit (zero-current) conditions. The sensor is made of separate, homogeneous, ionically conducting phases that form well-defined interfaces. These interfaces are unblocked for ionic charge-transfer processes (i.e. faradaic currents). The sensor's phases have standard chemical potentials of all the components and ionic mobilities in each phase constant in space and time. [3]

The driving forces for ion fluxes are gradients of ion concentrations and electric potentials. Pressure and temperature in modelled systems are assumed to be constant and osmotic effects (solvent flow) are ignored.

2.1. Phase Boundary Model

An interface between two liquid or solid phases represents a potential generating system. The phase-boundary potential or interfacial potential difference is caused mainly by the non-uniform distribution of electrically charged species between two phases and differences in single-ion chemical standard potentials. Donnan [36,37] was the first one to formulate the equilibrium between two electrolyte solutions separated by a membrane, having the capability to completely prevent the permeation of at least on kind of ion, therefore the boundary potential difference is often referred to as "Donnan term".

Phase Boundary Model (PBM) is based on two main assumptions:

1) The electroneutrality assumption: Migration effects are ignored; therefore, the kinetic parameters of all the ions involved are equal. That leads to the electroneutrality in the membrane, except the boundary. The membrane response is governed by the potential at the phase boundary - interface sample | membrane.

2) The total equilibrium assumption: At the membrane interface the electrochemical equilibrium is assumed. Difference in the inner electrical potentials φ_M balances the difference in the chemical potential for any ion that can be transported through the phase-boundary. Value φ_M is known as equilibrium potential. Additionally, both electrical potential and concentrations are constant in time and space (except the boundaries), which means there is no concentration drop over distance in the respective phases.

Using these two assumptions, Guggenheim developed a concept of electrochemical potential [38], that can be implemented as follows:

$$\tilde{\mu}_i = \mu_i + z_i F\varphi = \mu_i^0 + RT\ln(a_i) + z_i F\varphi, \quad (1)$$

where $\tilde{\mu}_i$ represents the electrochemical potential in the phase, μ_i is the chemical potential, μ_i^0 - chemical potential under standard conditions and φ is the electrical potential, a_i represents single free ion activity and z_i is its charge. *R, T, F* represents gas constant, absolute temperature and Faraday constant respectively.

To derive the phase boundary potential φ_{PB} as a function of concentration using Guggenheim's concept, several further assumptions have to be made. These assumptions are:

- The ideal selectivity assumption - only the *i*-th ion can transfer through the interface;
- The infinite kinetics assumption - ion transfer is fast and reversible;

- The ideal immiscibility assumption - phases are immiscible and have different chemical properties;
- The ideal phase assumption – convention for a single ion activity is used instead of a mean ionic activity, therefore the activity is assumed to be equal to concentration;
- The solvent impermeability assumption – there is no flux of solvent through the membrane.

Using eq. 1, the above assumptions and the condition of chemical equilibrium between two chemically different phases, it is possible to derive the equation for the electrical potential difference at the phase boundary:

$$\varphi_M = \varphi_{PB} = \frac{RT}{z_i F}\ln\left(k_i\right) + \frac{RT}{z_i F}\ln\left(\frac{c_i^S}{c_i^M}\right), \tag{2}$$

where c_i^S and c_i^M represent the concentration of the *i*-th ion in the bulk of sample solution and the membrane phase respectively and k_i is the ion-partition constant and is defined as $k_i = \exp\left(\frac{\mu_i^{0(S)} - \mu_i^{0(M)}}{RT}\right)$, where $\left(\mu_i^{0(S)} - \mu_i^{0(M)}\right)$ represents the difference in standard chemical potentials in respective phases.

First Phase-Boundary Model was described in 1937 by Nikolsky [39]. He was considering a pH-sensitive glass membrane in contact with the bathing solution containing H^+ as the preferred ions and Na^+ as the discriminated ones. The membrane potential was derived to take a form:

$$\varphi_M = \varphi_{PB} = const + \frac{RT}{z_i F}\ln\left(c_1^S + K_{IJ}c_2^S\right), \tag{3}$$

where c_1^S and c_2^S are the sample solution concentrations of preferred and discriminated ion, respectively and K_{IJ} represents the equilibrium constant for the ion exchange reaction $I^{+(M)} + J^{+(S)} \rightleftarrows I^{+(S)} + J^{+(M)}$, i.e. :

$$K_{IJ} = \frac{k_2}{k_1} = \frac{c_1^S c_2^M}{c_1^M c_2^S} \tag{4}$$

Three decades later Eisenman in his work [40] included the information about the different mobilities of ions and therefore extended the Nikolsky's equation for non-zero diffusion potential in the membrane, i.e. $\varphi_D \neq 0$. He considered cases with and without the association between ions in the membrane, as well as different membrane types, namely solid-state, glass, membranes containing ion exchangers and membranes containing ligands.

The equation describing a case of a membrane with fully dissociated ion-exchanger takes the form:

$$\varphi_M = \varphi_{PB} + \varphi_D = const + \frac{RT}{z_1 F}\ln\left(c_1^S + \frac{u_2}{u_1}K_{IJ}c_2^S\right) = const + \frac{RT}{z_1 F}\ln\left(c_1^S + \frac{D_2}{D_1}K_{IJ}c_2^S\right), \quad (5)$$

where u_1 and u_2 represents mobilities and D_1 and D_2 are the diffusion coefficients of respective ions.

Above models have been widely applied for the description of various sensors [14,15].

Nikolsky's and Eisenman's models provide analytical derivation of equations, possible only for two ions (preferred and discriminated) with equal charges. Analytical derivation of the equations for the description of membrane potential for ions with unequal charges is impossible in the frame of total equilibrium model [41,42,43,44]. To cover such cases, semi-empirical equations in the form similar to presented by Nikolsky or Eisenman can be used.

By the arbitral decision of IUPAC, a general equation for all ISE, covering all charges of ions, was developed [34]. This equation is widely known in electrochemistry as Nikolsky-Eisenman (NE) equation and is given as:

$$\varphi_M = const + \frac{RT}{z_1 F}\ln\left(c_1^S + K_{IJ}^{pot}(c_2^S)^{z_1/z_2}\right). \quad (6)$$

This semi-empirical equation can be extended further in order to include the lower detection limit (L) of ISE [45]. The extended equation takes the form:

$$\varphi_M = const + \frac{RT}{z_1 F}\ln\left(c_1^S + K_{IJ}^{pot}(c_2^S)^{z_1/z_2} + L\right). \quad (7)$$

Parameters K_{IJ}^{pot} and L are relevant for analytical practice, as well as the theoretical modelling. Theoretical modelling can also help to predict their values. Selectivity (K_{IJ}^{pot}) and detection limit are constitutive parameters of all ion-selective electrodes.

2.2. Diffusion Layer Models

PBM is based on a prejudicial claim, that "the transport through the membrane produces no electrical potential…" [46]. While Donnan equilibrium plays important role in the regulation of interfacial processes, such equilibria are usually not attained in the interior of the membranes. Thus, free energies of the species in the membrane, as well as the analyzed solution, undergo variations in space and time and the corresponding electrochemical potential gradients give rise to diffusional fluxes of ions.

The base of Diffusion Layer Models (DLM) is the local equilibrium assumption (it means that the equations derived by Nikolsky and Eisenman can be applied by substitution of bulk concentration of ions with the respective surface concentrations). Additionally, it is assumed that the sensor is in steady state, meaning that the concentrations of ions in the ion-selective membrane, as well as in the neighbouring phases, are dependent on distance, but independent on time.

The first DLM was created by Lewenstam [47], to model changes of selectivity coefficients with concentrations and time, and developed in his further works [48,49,50]. The equations developed by Guggenheim, Nikolsky and Eisenman (equations 1 to 6) with the bulk concentrations substituted by the surface (local) concentrations are the starting point for this model. Steady state ion fluxes are given by the linear concentration gradients between the boundaries and respective bulks. The diffusion layer is assumed to be constant and time-independent.

The time-dependent response for two ions of equal charge can be obtained by using a pivotal parameter *s(t)*. This parameter, known as the surface coverage or site filling factor, is characterizing the distance of the system under local equilibrium from the total equilibrium over time and is defined as:

$$s(t) = \frac{c_{j0}^{M}(t)}{c_{i0}^{M}(t) + c_{j0}^{M}(t)} = \frac{K_{IJ} c_{j0}^{S}(t)}{c_{i0}^{S}(t) + c_{j0}^{S}(t)}, \tag{8}$$

where $c_{i0}^{M}(t)$ and $c_{j0}^{M}(t)$ are the ion concentrations in the membrane at the interface membrane | solution at time *t*, $c_{i0}^{S}(t)$ and $c_{j0}^{S}(t)$ are the ion concentrations in the sample solution at this interface at time *t*. For the steady state as well as for the total equilibrium the pivotal parameter is given as:

$$s_{eq} = s(t \to \infty) = \frac{c_{j0}^{M}(t \to \infty)}{c_{i0}^{M}(t \to \infty) + c_{j0}^{M}(t \to \infty)} = \frac{K_{IJ} c_j^S}{c_i^S + K_{IJ} c_j^S}. \tag{9}$$

The concentration changes in the diffusion layer, with constant thickness *d*, are assumed to be linear (Nernst approach). By coupling the ion fluxes through the interface, J_i and J_j, using the mass conservation law, one obtains:

$$J_j = -J_i \;\Rightarrow\; D_j^S \frac{c_j^S - c_{j0}^S(t)}{d} = D_i^S \frac{c_{i0}^S(t) - c_i^S}{d}. \tag{10}$$

Combining equations 4, 5, 9 and 10 leads to obtaining the equation for the membrane potential in the following form:

$$\varphi_M(t) = const + \frac{RT}{z_i F} \ln \left\{ \frac{\left[1 - s(t)\right] K_{IJ} + s(t) \frac{D_j^M}{D_i^M} K_{IJ}}{\left[1 - s(t)\right] K_{IJ} + s(t) \frac{D_j^S}{D_i^S}} \cdot \frac{c_i^S + \frac{D_j^S}{D_i^S} c_j^S}{c_i^M} \right\}, \tag{11}$$

where D_i^M, D_j^M, D_i^S, D_j^S represent the diffusion coefficients of preferred and discriminated ion in the membrane and diffusion layer (solution) respectively.

Separation of the variables *s(t)* and *t* and integrating within the time limits *t* to $t = \infty$ and corresponding *s* limits *s(t)* to $s_{eq} = s(t \to \infty)$, leads to obtaining the function binding *s(t)* and *t* in the form:

$$\left(K_{IJ} - \frac{D_j^S}{D_i^S} \right) s(t) - K_{IJ} \frac{c_i^S + \frac{D_j^S}{D_i^S} c_j^S}{c_i^S + K_{IJ} c_j^S} \ln \left(1 - \frac{s(t)}{s_{eq}} \right) = \left(c_i^S + K_{IJ} c_j^S \right) \cdot \frac{D_j^S A}{n_{tot} d} t, \tag{12}$$

where *A* is the electrode surface and n_{tot} is the total number of sites on the membranes surface occupied by the ions [51].

It is worth mentioning that the time in DLM is given as the ad hoc parameter to describe the equilibration (reaching the equilibrium) via diffusion controlled transport. The DLM predicts that the selectivity coefficient K_{IJ}^{pot} as given in the Nikolsky-Eisenman equation (eq. 6) changes during this process between two limiting values [49-52]. The first of these values for a short response time is dictated by the ion transport of the solution

$$K_{IJ}^{pot}\left(t \to 0\right) = \frac{D_j^S}{D_i^S} \approx 1, \tag{13}$$

while the second one corresponds to steady state or total equilibrium

$$K_{IJ}^{pot}\left(t \to \infty\right) = \frac{D_j^M}{D_i^M} K_{IJ}. \tag{14}$$

The prediction given by eq. 13 has been used in practice to kinetically discriminate strong interferences by applying short readout times [53,54] or to benefit the measurements of strongly interfering ions, e.g. heparin on chloride-selective electrodes [55,56].

The main frame of DLM was further developed by Sokalski et al. [57]. The authors took into consideration not only the ion exchange, but also coextraction process in steady state. Presented approach allows the description of the lower detection limit of ISE [58] and its dependence on the various parameters, especially concentrations of ions in the inner solution. Another more general steady-state model based on DLM frame was developed by Morf et al. [42] and considers arbitrary number of ions of any charge. These two models give identical results.

More details considering the models presented above and their applications and limitations can be found in publication I and in the chapter 3.3. of this thesis.

2.3. Time-dependency

Although DLM includes time as one of the parameters, direct computation of the electrode potential (i.e. by obtaining the pivotal parameter *s(t)* using eq. 12) for the transient states are rather complicated, namely due to the unknown value of total number of sites at the membrane surface n_{tot}. Time-dependency can be either obtained by including time as an artificial parameter [42] or by expressing diffusion using a time-dependent Cauchy problem with suitable initial and boundary condition [59].

The Cauchy problem was formulated by assuming pure diffusion inside both the diffusion layer and the membrane, where the concentration change of the *i*-th ion inside the *j*-th layer is given by the continuity equation and Fick's first law:

$$\begin{cases} \dfrac{\partial c_i^j}{\partial t}(x,t) = -\dfrac{\partial J_i^j}{\partial x}(x,t) = -D_i^j \dfrac{\partial^2 c_i^j}{\partial x^2}(x,t) \\ x \in]\lambda_{j-1}, \lambda_j[\quad \text{for each phase } j = 1,\ldots,n \\ t \in [0, t_{END}] \end{cases} \tag{15}$$

where c_i^j represents concentration of the *i*-th ion in the *j*-th phase, λ_{j-1} and λ_j represent the boundaries of the *j*-th phase. The solution of this equation is a base for various calculations in diffusion science and materials engineering [60,61,62].

Two phases, namely phase 1 - aqueous diffusion layer and phase 2 - the ion-selective membrane are considered. The Finite Difference Method for two separate uniform grids for the space domain and Euler's method to solve the set of obtained ODEs are used. At each time step, the concentration of the *i*-th ion in the *k*-th discretization point of the *j*-th layer $c_i^{j,k}(t+\Delta t)$ is expressed as:

$$c_i^{j,k}(t+\Delta t) = c_i^{j,k}(t) + \frac{D_i^j}{\delta_j^{\,2}}(c_i^{j,k-1}(t) - 2c_i^{j,k}(t) + c_i^{j,k+1}(t))\Delta t, \tag{16}$$

where $\delta^j = \dfrac{d_j}{N_j - 1}$ represents the distance between two neighbouring grid points.

Eq. 16 has to be accompanied with proper boundary conditions. At the membrane boundaries, the ion the concentrations of the preferred and discriminated ions are given by the equations for equilibrium distribution:

$$c_1^{2,0}(t+\Delta t)=\frac{\mathrm{R_T}c_1^{1,N}(t+\Delta t)}{c_1^{1,N}(t+\Delta t)+K_{exch}c_2^{1,N}(t+\Delta t)},\qquad c_2^{2,0}(t+\Delta t)=\mathrm{R_T}-c_1^{2,0}(t+\Delta t)$$
$$c_1^{2,N}(t+\Delta t)=\frac{\mathrm{R_T}c_{1,R}}{c_{1R}+K_{exch}c_{2R}},\qquad c_2^{2,N}(t+\Delta t)=\mathrm{R_T}-c_1^{2,N}(t+\Delta t) \tag{17}$$

where $\mathrm{R_T}$ is the total concentration of anionic sites in the membrane and K_{exch} is the exchange constant and c_{iR} represents the concentration of the *i*-th ion in the inner solution.

At the boundary solution bulk | diffusion layer Dirichlet boundary conditions, i.e. $c_i^1(\lambda_0,t)=c_{iL}=const$, are used and the concentrations in the diffusion layer at the interface with the membrane are given by the continuity equation:

$$c_i^{1,N}(t+\Delta t)=c_i^{1,N}(t)+\frac{2D_i^1}{\delta_1(\delta_1+\delta_2)}(c_i^{1,N-1}(t)-c_i^{1,N}(t))\Delta t+\frac{2D_i^2}{\delta_2(\delta_1+\delta_2)}(c_i^{2,1}(t)-c_i^{2,0}(t))\Delta t. \tag{18}$$

Finally, the resulting potential of the ISE is calculated according to the well-known Nikolsky-Eisenman equation in the form:

$$\varphi=\frac{RT}{F}\ln\frac{c_1^{1,N}+K_{exch}c_2^{1,N}}{c_{1R}+K_{exch}c_{2R}}. \tag{19}$$

The model described above [59] does not take into account the coextraction process, therefore cannot be used to describe properly the effect of lower detection limit caused by leakage of the preferred ion to the diffusion layer [58]. To make such description, possible eq. 17 has to be substituted by:

$$c_1^{2,0}(t)=\frac{\mathrm{R_T}+\sqrt{\Delta_1}}{2+2K_{exch}\dfrac{c_2^{1,N}(t)}{c_1^{1,N}(t)}},\qquad c_2^{2,0}(t)=c_1^{2,0}(t)K_{exch}\frac{c_2^{1,N}(t)}{c_1^{1,N}(t)}$$
$$c_1^{2,N}(t)=\frac{\mathrm{R_T}+\sqrt{\Delta_2}}{2+2K_{exch}\dfrac{c_{2R}}{c_{1R}}},\qquad c_2^{2,N}(t)=c_1^{2,N}(t)K_{exch}\frac{c_{2R}}{c_{1R}} \tag{20}$$

where:

$$\Delta_1=\mathrm{R_T}^2+4\left(1+K_{exch}\frac{c_2^{1,N}(t)}{c_1^{1,N}(t)}\right)\left(c_1^{1,N}(t)+c_2^{1,N}(t)\right)c_1^{1,N}(t)K_{coex}$$
$$\Delta_2=\mathrm{R_T}^2+4\left(1+K_{exch}\frac{c_{2R}}{c_{1R}}\right)\left(c_{1R}+c_{2R}\right)c_{1R}K_{coex} \tag{21}$$

where K_{coex} represents the coextraction constant.

More details considering the time-dependent exchange model (TDM-E), described with the equations 16-19, as well as the time-dependent exchange-coextraction model (TDM-EC), described with equations 16 and 19-21, can be found in publication I.

A very interesting, but mathematically way more complicated time-dependent model based on the Diffusion Layer approach was presented by Radu et al. [63]. The model is based on a numerical method using finite difference discretization in time and finite element discretization in space, giving an approximate solution of the diffusion equation in the diffusion layer and the membrane. It treats the interface between the membrane and the sample on the basis of current ion-exchange and ISE selectivity theory, leading to a one-dimensional transmission problem with a non-linear jump condition on the interface.

2.4. Nernst-Planck-Poisson Model

All of the models described above share three main assumptions:

1) The potential is governed by the local equilibria described by the Nikolsky-Eisenman equation (eq. 6).

2) Only the Fickian diffusion is considered, i.e. the only source of ion fluxes is the concentration gradient (migration is ignored), which is a rough approximation, since ions are charged and therefore both create and interact with an electrical field.

3) The electroneutrality is assumed. While in some cases using the electroneutrality condition is justified, there are many others where this assumption is overused. The reason for using this assumption is that it produces a problem, which is much easier to solve. Historically, such a simplification was almost necessary due to the lack of high performing computers. But this attitude cannot be defended now, when the access to high computing power is widespread. Furthermore, in the recent work of Perram et. al. [64] this assumption was denounced as unphysical (electroneutrality at finite time is dynamically inconsistent with solutions where the Poisson equation is obeyed).

Consequently, the models presented in previous chapters fail in many situations [44]. In order to avoid these approximations, more advanced modelling is required. This can be performed by adopting the Nernst-Planck-Poisson (NPP) equations system, which is general and rich enough in a physical sense to describe the generation of the membrane potential.

Taking migration into account can be achieved by using the Nernst – Planck (NP) flux expression, which describes the flux of ions in space and time:

$$J_i^j(x,t) = -D_i^j \frac{\partial c_i^j}{\partial x}(x,t) - \frac{F}{RT} D_i^j z_i (c_i^j E^j)(x,t) + (c_i^j \upsilon^j)(x,t), \tag{22}$$

where $\upsilon^j(x,t)$ is the drift velocity. The above equation connects the flux with three processes: diffusion $-D_i^j \frac{\partial c_i^j}{\partial x}(x,t)$, migration $-\frac{F}{RT} D_i^j z_i (c_i^j E^j)(x,t)$ and drift $+(c_i^j \upsilon^j)(x,t)$.

Gauss's law (or equivalently Poisson equation if electric potential instead of electric field is used) in the form:

$$\frac{\partial E^j(x,t)}{\partial x} = -\frac{\partial^2 \varphi^j(x,t)}{\partial x^2} = \frac{F}{\varepsilon_j} \sum_i z_i c_i^j(x,t) \tag{23}$$

can be substituted with the total current equation, given by Cohen and Cooley [65]:

$$I(t) = F \cdot \sum_{i=1}^{r} z_i J_i^j(x,t) + \varepsilon_j \cdot \frac{\partial E^j(x,t)}{\partial t}, \tag{24}$$

where $I(t)$ is current density and is a constant or time-dependent function.

To connect concentrations evolution in time with flux of components mass balance equation

$$\frac{\partial c_i^j}{\partial t} = -\frac{\partial J_i^j}{\partial x} \tag{25}$$

is used.

Finally, the electrical potential is calculated as the integral of electric field over space:

$$\Delta\varphi^j = -\int_{\lambda_{j-1}}^{\lambda_j} E^j(x,t)dx, \tag{26}$$

where λ_{j-1} and λ_j represent the phase boundaries.

Equations 22-25, accompanied by proper initial and boundary conditions described in detail in the chapter 3.1., form a set of partial differential equations PDEs. Solution of these equations allows obtaining the concentration and electrical fields as the functions of space and time. Integration of electrical field using eq. 26 leads to obtaining the potential as a function of time.

The amount of various assumptions made in the NPP model is lower than in the total equilibrium models (PBMs) or the local equilibrium models (DLMs). The assumptions made are shared with all of the previously presented models and include:

- the dielectric permittivity and diffusion coefficients have no dependence on concentrations,
- activities are equal to concentrations (ideal solutions, i.e. activity coefficients are equal to 1)
- no reaction terms (except the case presented in chapter 3.4., where an extension to NPP model is presented).
- one dimensional geometry (with the exception for the work of Samson et al. [66])

2.5. Historical Solutions of NPP

The first solution of the Nernst-Planck equation was obtained in 1890 by Planck himself [67]. He considered the steady-state one-dimensional diffusion of two monovalent ions through a membrane, using the electroneutrality and zero current assumptions. More than a half century later Schlögl [68], using the same assumptions, extended this analytical solution for the description of arbitrary number of ions of any valence number. Also, using the same assumptions, Conti and Eisenman [31] proposed a different solution applicable also for transient-state problems.

Other analytical solutions of NPP problem were presented by Helfferich [69] and Teorrel [70], who assumed the electroneutrality and by Goldman [71], who assumed the constant electric field across the membrane. Electroneutrality assumption and constant field hypothesis are just particular applications of the Poisson equation [72,73] (first applicable only for high concentrations and the latter valid rather for low concentrations). The difficulties of solving the NPP problem analytically and the search for more the more general and widely applicable solution, led researchers to use the numerical methods.

Explicit (non-predictive) and implicit (predictive) numerical methods for solving "analytically unsolvable" systems of coupled nonlinear partial differential equations were first proposed in the 1950s alongside with arrival of digital computers. The first numerical procedure for the simulation of time dependent NPP problem using an explicit method was developed in 1965 by Cohen and Cooley [65]. A decade later, a mixed implicit method (for electric field) and an explicit method (for concentrations) similar to [65] was presented by Sandifer and Buck [74]. Unfortunately, due to the explicit nature of the concentration calculation, their methods suffered from a very small time step of integration and therefore were very time-consuming.

The system of NPP equations is multidisciplinary, appearing in many fields of science and technology where the charge transport occurs. It finds application in semiconductors [75], building materials (such as concrete) [76], synthetic and biological charged membranes [77] and colloids [78]. Particularly interesting method used in the field of semiconductors is the implicit method, put forward by Scharfetter and Gummel [79]. They developed an improved flux equation obtained by integration of the Nernst-Planck equation, while the flux and electric field were held constant in each volume element. They performed the time step integration using Crank-Nicolson method [80]. Many of the semiconductor-

oriented procedures, although quite powerful, are dedicated to specific problems (usually with the restriction to two mobile charge carriers).

A substantial contribution to the numerical treatment of NPP with applications to membrane electrochemistry is a work of Brumleve and Buck [81], who developed an efficient finite difference simulation procedure for multi-component NPP equations using fully implicit time scheme that was subsequently solved by the implicit iterative Newton-Raphson technique [82] coupled to Gaussian elimination. This fundamental work was later taken up and continued by several groups, including contributions by Mafé, Pellicer, Manzanares and Kontturi [83,84,85,86,87], as well as the ones by Lewenstam and Sokalski [35,44,88,89]. An approach, based upon this idea and dedicated to the general description of ISE behaviour and developed in numerous papers, is also followed in this thesis.

In 1992 Murphy et al. [90] presented an NPP model with Butler-Volmer boundary conditions [91]. This type of conditions used to describe electrode kinetics takes into account the structure of non-equilibrium electrical double layer. They used the Method of Lines (MoL) [92] for space discretization and Gear's stiffly stable predictor-corrector method [93] (namely LSODI package [94]) to solve the resulting differential-algebraic system of equations. This model can be useful for the description of the ion transport, where large gradients in the physical variables occur, e.g. through inhomogeneous materials like bipolar [95] and asymmetric membranes [84]. Another approach based on the Method of Lines, but with the Chang-Jaffé boundary conditions, was presented by Filipek [96] and compared with the solution based on Finite Elements Method (FEM). Results obtained using MoL and FEM are in the good agreement.

Historically it was assumed that the potential formation occurs only in the membrane phase, therefore, in all previously mentioned works only one layer was considered. The first extension of the NPP model for a two layer system was presented in [97]. Later on, the NPP model for an arbitrary number of layers was developed and implemented in C++ programming language [98], as well as in MathCad [99] and Matlab [100] scripts.

The NPP solutions, presented in [35], [44], [88]-[89] and [96]-[100], are using Chang-Jaffé boundary conditions [101], which are a simplification of the Butler-Volmer conditions. All of these methods use the method of lines for space discretization, which results in a set of stiff Ordinary Differential Equations (ODEs), which can be solved using special numerical integrators (see chapter 3.1.2. and 3.1.3. for more details).

All above works present the solution of the NPP model in one-dimensional geometry. In 1996 Harden and Viovy [102] presented a method that can be easily transposed in two-

or three-dimensional geometry. The first numerical scheme working in two-dimensional geometry (and easily extendable for 3D cases) was presented three years later by Samson et al. [66]. They developed a method based on Newton-Raphson technique [82] and used it to investigate effect of the presence of electrical charges on the inner surface of a pore. The geometries of more than one dimension are out of the scope of this thesis.

3. Results and Discussion

3.1. NPP Modelling for Arbitrary Number of Layers

Let us consider a system that consists of *n* layers, each representing different phase, inside of which concentration changes of *r* components c_i^j (ions or uncharged chemical species) and a change of the electrical field E^j in space and time takes place. The scheme of the *n*-layer system is presented in Fig. 2.

Each layer has its own thickness d_j and dielectric permittivity ε_j, is flat and isotropic, so it can be assumed as a continuous environment. On the right and the left side of that system of layers, the bulk solutions with constant concentrations of each component, c_{iR} and c_{iL}, is assumed.

The system has a constant temperature *T*. The charge z_i of each ion *i* and diffusion coefficients D_i^j in each layer α_j, are known. External current *I(t)* can be applied to the system.

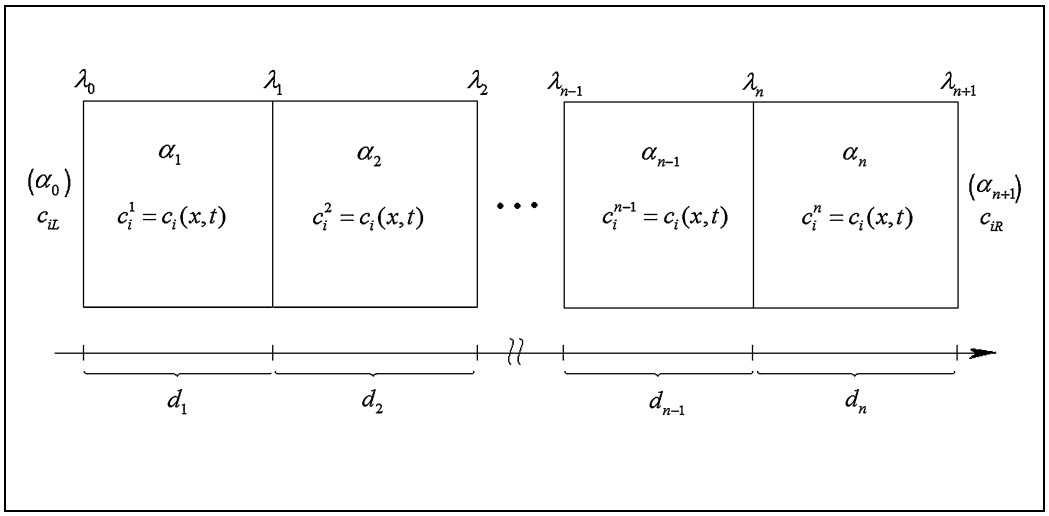

Figure 2. *The scheme of the n-layer system between two solutions with i-th component concentration* c_{iL} *on the left, and* c_{iR} *on the right side of the system*

The influence of diffusion and migration is expressed by the Nernst-Planck equation (eq. 22). The continuity equation (eq. 25) describes the change of the ion concentrations in time, and the displacement current equation (eq.24) describes the electrical changes caused by the interaction of the species.

Electrical potential in space for each layer can be calculated from eq. 26 and the overall electrical potential in the system is a sum of the electrical potentials in all layers:

$$\Delta\varphi = \sum_{j=1}^{n} \Delta\varphi^{j}(\lambda_j) = -\sum_{j=1}^{n} \int_{\lambda_{j-1}}^{\lambda_j} E^{j}(x,t)dx. \tag{27}$$

The values of fluxes at the boundaries (the interface λ_j between layers α_j and α_{j+1}) are calculated using modified (with concentrations as variables, not constants) Chang-Jaffe [101] conditions in the form:

$$J_i^j(\lambda_j,t) = J_i^{j+1}(\lambda_j,t) = \overrightarrow{k_{i\lambda_j}} c_i^j(\lambda_j,t) - \overleftarrow{k_{i\lambda_j}} c_i^{j+1}(\lambda_j,t), \tag{28}$$

where $\overrightarrow{k_{i\lambda_j}}, \overleftarrow{k_{i\lambda_j}}$ are the first order heterogeneous rate constants used to describe the interfacial kinetics. The $\overrightarrow{k_{i\lambda_j}}$ constant corresponds to the ion *i*, which moves from layer α_j to α_{j+1}, and $\overleftarrow{k_{i\lambda_j}}$ - to the ion *i*, which moves from α_{j+1} to α_j. The Chang-Jaffe conditions correspond to the Butler-Volmer conditions with zero overpotential.

Boundary points $x = \lambda_j$ are specific points in space, which have a neighbourhood in two different layers. Due to this fact, two separate values of each ion concentration $c_i^j(\lambda_j,t)$ and $c_i^{j+1}(\lambda_j,t)$, as well as two separate values of electrical field $E^j(\lambda_j,t)$ and $E^{j+1}(\lambda_j,t)$, should be considered. The concentrations on the left and right side of the system are expressed as $c_i^0(\lambda_0,t) = c_{iL}$ and $c_i^{n+1}(\lambda_n,t) = c_{iR}$, where c_{iL} and c_{iR} are constants.

Change-Jaffe boundary conditions for fluxes and standard Dirichlet conditions for concentrations values were compared in publication III. It was demonstrated that for large heterogeneous rate constants ($\overrightarrow{k_{i\lambda_j}} > 100\, m\cdot s^{-1}$ and $\overleftarrow{k_{i\lambda_j}} > 100\, m\cdot s^{-1}$ in the Chang-Jaffe boundary conditions – eq. 28) solutions of NPP problem are consistent with those obtained for the Dirichlet boundary conditions for concentrations. Thus, boundary conditions used in presented model are more general than the Dirichlet conditions, therefore give a wider range of applications.

For completeness, the above system must be accompanied by initial conditions. The implementation presented in this thesis allows us to use three types of initial conditions:

- flat-band condition with constant concentration in each layer: $c_i^j(0,x) = const$ and $E^j(0,x) = 0$,
- concentration profiles obtained during calibration process,
- concentration profiles obtained from previous simulations.

The equations 22-25 and 28 form the following system of nonlinear partial differential equations (PDEs) for *r* components:

$$\begin{cases} \dfrac{\partial c_i^j}{\partial t}(x,t) = -\dfrac{\partial J_i^j}{\partial x}(x,t) \ \text{ for } \ i = 1,\ldots,r; \\ \dfrac{\partial E^j}{\partial t}(x,t) = \dfrac{1}{\varepsilon_j} I(t) - \dfrac{F}{\varepsilon_j} \sum_{i=1}^{r} z_i J_i^j(x,t); \\ x \in [\lambda_{j-1}, \lambda_j] \ \text{ for each phase } \ j = 1,\ldots,n; \\ t \in [0, t_{END}] \end{cases} \tag{29}$$

where the expressions for flux J_i are:

- $J_i^j(x,t) = -D_i^j \dfrac{\partial c_i^j}{\partial x}(x,t) - \dfrac{F}{RT} D_i^j z_i (c_i^j E^j)(x,t) + (c_i^j \upsilon^j)(x,t)$ inside the layers,
- $J_i^j(\lambda_j,t) = J_i^{j+1}(\lambda_j,t) = \overrightarrow{k_{i\lambda_j}} c_i^j(\lambda_j,t) - \overleftarrow{k_{i\lambda_j}} c_i^{j+1}(\lambda_j,t)$ at the boundaries.

By solving this set of PDEs, the distribution of concentrations and electrical field for any time $t > 0$ is obtained, and electrical potential can be calculated (using eq. 27).

For simplicity, the convection part of the flux expression is neglected, i.e. $(c_i^j \upsilon^j)(x,t) = 0$, as the calculation of drift is out of the scope of this thesis. For details concerning calculations of convection, including its influence on the system, see [103].

3.1.1. Rescaling of the Problem

Different time and space scales for diffusion (very slow process) and migration (quick process) create the necessity of rescaling the variables [65]. To achieve this aim, new dimensionless variables have to be introduced, using the following transformations:

$$\bar{x} = \frac{x}{x_s}, \quad \overline{\lambda_j} = \frac{\lambda_j}{x_s}, \quad \bar{t} = \frac{t}{t_s}, \quad \overline{c_i^j}\left(\bar{x},\bar{t}\right) = \frac{c_i^j\left(x_s\bar{x},t_s\bar{t}\right)}{c_s}, \quad \overline{E^j}\left(\bar{x},\bar{t}\right) = \frac{E^j\left(x_s\bar{x},t_s\bar{t}\right)}{E_s} \tag{30}$$

where x_s, t_s, c_s, E_s are characteristic constants (scaling factors).

Using these transformations, one can express the derivatives of concentrations and electrical field:

$$\begin{aligned}
&\frac{\partial c_i}{\partial t} = \frac{\partial\left(c_s\overline{c_i}\right)}{\partial\bar{t}}\frac{\partial\bar{t}}{\partial t} = \frac{c_s}{t_s}\frac{\partial\overline{c_i}}{\partial\bar{t}}\\
&\frac{\partial E}{\partial t} = \frac{\partial\left(E_s\bar{E}\right)}{\partial\bar{t}}\frac{\partial\bar{t}}{\partial t} = \frac{E_s}{t_s}\frac{\partial\bar{E}}{\partial\bar{t}}\\
&\frac{\partial c_i}{\partial x} = \frac{\partial\left(c_s\overline{c_i}\right)}{\partial\bar{x}}\frac{\partial\bar{x}}{\partial x} = \frac{c_s}{x_s}\frac{\partial\overline{c_i}}{\partial\bar{x}}\\
&\frac{\partial}{\partial x} = \frac{\partial}{\partial\bar{x}}\frac{\partial\bar{x}}{\partial x} = \frac{1}{x_s}\frac{\partial}{\partial\bar{x}}
\end{aligned} \tag{31}$$

Now the set of PDEs (29) can be rewritten using new rescaled variables:

$$\begin{cases}
\dfrac{c_s}{t_s}\dfrac{\partial\overline{c_i^j}}{\partial\bar{t}}\left(\bar{x},\bar{t}\right) = -\dfrac{\partial}{\partial x}\left(\dfrac{J_i^j\left(x_s\bar{x},t_s\bar{t}\right)}{x_s}\right) \text{ for } i = 1,\ldots,r;\\
\dfrac{E_s}{t_s}\dfrac{\partial\overline{E^j}}{\partial\bar{t}}\left(\bar{x},\bar{t}\right) = \dfrac{1}{\varepsilon_j}I(t_s\bar{t}) - \dfrac{F}{\varepsilon_j}\sum_{i=1}^{r} z_i J_i^j\left(x_s\bar{x},t_s\bar{t}\right).
\end{cases} \tag{32}$$

Flux of components (equation 22) can be expressed by:

$$J_i^j(x,t) = -\frac{c_s}{x_s}D_i^j\frac{d\overline{c_i^j}}{d\bar{x}}\left(\frac{x}{x_s},\frac{t}{t_s}\right) - c_s E_s\frac{F}{RT}D_i^j z_i(\overline{c_i^j}\,\overline{E^j})\left(\frac{x}{x_s},\frac{t}{t_s}\right). \tag{33}$$

By transforming above equations we get:

$$\begin{cases}
\dfrac{\partial\overline{c_i^j}}{\partial\bar{t}}\left(\bar{x},\bar{t}\right) = -\dfrac{\partial}{\partial\bar{x}}\left(\dfrac{t_s}{c_s x_s}J_i^j\right)(x,t) = -\dfrac{\partial\overline{J_i^j}}{\partial x}\left(\bar{x},\bar{t}\right) \text{ for } i = 1,\ldots,r;\\
\dfrac{\partial\overline{E^j}}{\partial\bar{t}}\left(\bar{x},\bar{t}\right) = \dfrac{t_s}{E_s\varepsilon_j}I(t_s t) - \dfrac{t_s F}{E_s\varepsilon_j}\sum_{i=1}^{r} z_i J_i^j(x,t) = \overline{I^j}(\bar{t}) - \Lambda^j\sum_{i=1}^{r} z_i\overline{J_i^j}\left(\bar{x},\bar{t}\right),
\end{cases} \tag{34}$$

where Λ^j, rescaled current $\overline{I^j}$ and rescaled flux are defined as:

$$\Lambda^j = \frac{c_s x_s F}{E_s \varepsilon_j}, \qquad \overline{I^j}(\bar{t}) = \frac{t_s}{E_s \varepsilon_j} I(t_s \bar{t}),$$
$$\overline{J_i^j}(\bar{x},\bar{t}) = \frac{t_s}{c_s x_s} J_i^j(x_s \bar{x}, t_s \bar{t}) = -\frac{t_s}{x_s^{\,2}} D_i^j \frac{d\overline{c_i^j}}{d\bar{x}}(\bar{x},\bar{t}) - \frac{t_s E_s}{x_s} \frac{F}{RT} D_i^j z_i (\overline{c_i^j E^j})(\bar{x},\bar{t}). \tag{35}$$

Boundary conditions (eq. 28) take the form:

$$\overline{J_i^j}(\overline{\lambda_j},\bar{t}) = \overline{J_i^{j+1}}(\overline{\lambda_j},\bar{t}) = \frac{t_s}{c_s x_s} J_i^j(x_s \overline{\lambda_j}, t_s \bar{t}) = \frac{t_s}{x_s} \overrightarrow{k_{i\lambda_j}}\, \overline{c_i^j}(x_s \overline{\lambda_j}, t_s \bar{t}) - \frac{t_s}{x_s} \overleftarrow{k_{i\lambda_j}}\, \overline{c_i^{j+1}}(x_s \overline{\lambda_j}, t_s \bar{t}) \tag{36}$$

As a result of all above transformations, the set of PDEs (eq. 29) takes the form:

$$\begin{cases} \dfrac{\partial \overline{c_i^j}}{\partial \bar{t}}(\bar{x},\bar{t}) = -\dfrac{\partial \overline{J_i^j}}{\partial \bar{x}}(\bar{x},\bar{t}) \ \text{ for } \ i = 1,\ldots,r, \\ \dfrac{\partial \overline{E^j}}{\partial \bar{t}}(\bar{x},\bar{t}) = \overline{I^j}(\bar{t}) - \Lambda^j \sum_{i=1}^{r} z_i \overline{J_i^j}(\bar{x},\bar{t}), \\ \bar{x} \in [\overline{\lambda_{j-1}}, \overline{\lambda_j}], \\ \bar{t} \in \left[0, \dfrac{t_{END}}{t_c}\right], \end{cases} \tag{37}$$

where the *i*-th component flux at the boundaries can be expressed as

$$\overline{J_i^j}(\overline{\lambda_j},\bar{t}) = \overline{J_i^{j+1}}(\overline{\lambda_j},\bar{t}) = \overline{\overrightarrow{k_{i\lambda_j}}\, c_i^j}(\overline{\lambda_j},\bar{t}) - \overline{\overleftarrow{k_{i\lambda_j}}\, c_i^{j+1}}(\overline{\lambda_j},\bar{t}) \quad \text{for i = 1 ... r} \tag{38}$$

and the *i*-th component flux inside each layer can be expressed as

$$\overline{J_i^j}(\bar{x},\bar{t}) = -a_i^j \frac{d\overline{c_i^j}}{d\bar{x}}(\bar{x},\bar{t}) + b_i^j (\overline{c_i^j E^j})(\bar{x},\bar{t}) + \sum_{l=1}^{r} \left\{ g_l^j \left(\overline{c_i^j} \frac{\partial \overline{c_l^j}}{\partial \bar{x}} \right)(\bar{x},\bar{t}) \right\}. \tag{39}$$

In above equations some new constants were used. These new constants contain both physical and rescaling constants, and can be defined as:

$$a_i^j = \frac{t_s}{x_s^{\,2}} D_i^j, \quad b_i^j = \frac{t_s E_s}{x_s} \frac{F}{RT} D_i^j z_i, \quad g_l^j = \frac{t_s c_s}{c_{mixt} x_s^{\,2}} D_l^j,$$
$$\overline{\overrightarrow{k_{i\lambda_j}}} = \frac{t_s}{x_s} \overrightarrow{k_{i\lambda_j}}, \quad \overline{\overleftarrow{k_{l\lambda_j}}} = \frac{t_s}{x_s} \overleftarrow{k_{l\lambda_j}}\ . \tag{40}$$

Finally, the rescaled electrical potential in space and overall electrical potential in multi-layer system can be expressed as below:

$$\varphi^j(x) = x_s E_s \cdot \overline{\varphi^j}(\bar{x})\ ,$$
$$\Delta\varphi = x_s E_s \cdot \sum_{j=1}^{n} \overline{\varphi^j}(\overline{\lambda_j}) = -x_s E_s \cdot \sum_{j=1}^{n} \int_{\overline{\lambda_{j-1}}}^{\overline{\lambda_j}} \overline{E^j}(\bar{x}) d\bar{x}\ . \tag{41}$$

3.1.2. Numerical Method (Method of Lines) and Discretization

The set of PDEs, described by eq. 37, is impossible to solve analytically. Using Method of Lines (MoL) [104] we can transform it into the set of stiff ordinary differential equations (ODEs), which is then solved numerically by integrator.

The Method of Lines (one of the Finite Difference Methods) allows transformation of the set of PDEs into a set of ODEs. The method used to solve numerically the above problem requires space discretization only. That means some discrete points, with defined concentrations and fields (electric and fluxes) in space in each layer are chosen.

The non-uniform grid denser near boundaries presented in Fig. 3, is used. Because of grid non-uniformity the finite differences with properly selected weights must be applied [44,105]. For each layer α_j, the concentrations are defined at points $y_{j,k}$ (where $k = 0,\ldots,N_j+1$), while the fields at points $x_{j,k}$ $(k = 0,\ldots,N_j)$. Each two $x_{j,k}$ points are separated by a distance $h_{j,k} = x_{j,k+1} \div x_{j,k}$ and each point $y_{j,k}$ is placed in the middle of an interval $\left[x_{j,k-1}, x_{j,k}\right]$.

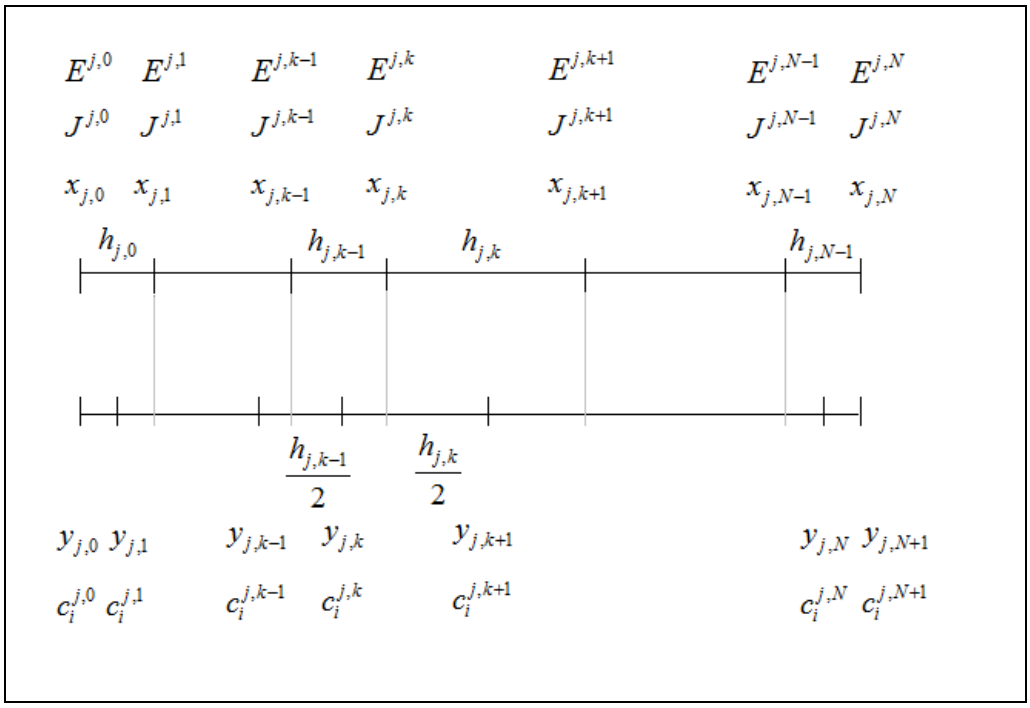

Figure 3. *The space grid in each layer used by computer program to solve the electro-diffusion problem.*

From this point on, rescaled variables are used in the equations and to simplify the burden of notation the overbars are dropped. The finite difference approximation of continuity equation which corresponds to the above grid for internal nodes reads:

$$\left.\frac{\partial c_i^j}{\partial t}\right|_{y_{j,k}} = -\left.\frac{\partial J_i^j}{\partial x}\right|_{y_{j,k}}, \tag{42}$$

where flux J_i^j gradient in point $y_{j,k}$ (for $k = 0,\ldots,N_j$) can be evaluated using expression for the first derivative:

$$\left.\frac{\partial J_i^j}{\partial x}\right|_{x_{j,k}} = \frac{J_i^{j,k} - J_i^{j,k-1}}{h_{j,k-1}}. \tag{43}$$

At the boundary nodes ($k = 0$ and $k = N_j + 1$) one sided expressions for right- and left-side derivative are used:

$$\begin{aligned}
\left.\frac{\partial J_i^j}{\partial x}\right|_{y_{j,0}} &\approx \frac{-h_{j,1}(2h_{j,0}+h_{j,1})J_i^{j,0} + (h_{j,0}+h_{j,1})^2 J_i^{j,1} - h_{j,0}^2 J_i^{j,2}}{h_{j,0}h_{j,1}(h_{j,0}+h_{j,1})}, \\
\left.\frac{\partial J_i^j}{\partial x}\right|_{y_{j,N_j+1}} &\approx \frac{h_{j,N_j-1}^2 J_i^{j,N_j-2} - (h_{j,N_j-1}+h_{j,N_j-2})^2 J_i^{j,N_j-1} + h_{j,N_j-2}(h_{j,N_j-2}+2h_{j,N_j-1})J_i^{j,N_j}}{h_{j,N_j-1}h_{j,N_j-2}(h_{j,N_j-2}+h_{j,N_j-1})}.
\end{aligned} \tag{44}$$

The finite difference approximation of displacement current equation corresponding to the above grid for all nodes reads:

$$\left.\frac{\partial E^j}{\partial t}\right|_{y_{j,k}} = I^j(t) - \Lambda^j \sum_{i=1}^{r} z_i J_i^{j,k}. \tag{45}$$

Combining equations 42 – 45, leads to formulating the set of ODEs defined with the unknown functions $c_i^{j,k}$, which have values in every point $y_{j,k}$ (where $k = 0,\ldots,N_j+1$) and $E^{j,k}$, which have values in every point $x_{j,k}$ (where $k = 0,\ldots,N_j$):

$$\begin{aligned}
\frac{dc_i^{j,0}}{dt} &= \frac{-h_{j,1}(2h_{j,0}+h_{j,1})J_i^{j,0} + (h_{j,0}+h_{j,1})^2 J_i^{j,1} - h_{j,0}^2 J_i^{j,2}}{h_{j,0}h_{j,1}(h_{j,0}+h_{j,1})}, \\
\frac{dc_i^{j,k}}{dt} &= -\frac{J_i^{j,k} - J_i^{j,k-1}}{h_{j,k-1}}, \\
\frac{dc_i^{j,N_j+1}}{dt} &= \frac{h_{j,N_j}^2 J_i^{j,N_j-1} - (h_{j,N_j-1}+h_{j,N_j})^2 J_i^{j,N_j} + h_{j,N_j}(h_{j,N_j}+2h_{j,N_j-1})J_i^{j,N_j+1}}{h_{j,N_j-1}h_{j,N_j}(h_{j,N_j-1}+h_{j,N_j})}, \\
\frac{dE_i^{j,k}}{\partial t} &= I^j(t) - \Lambda^j \sum_{i=1}^{r} z_i J_i^{j,k},
\end{aligned} \tag{46}$$

where the value of *i*-th component's flux $J_i^{j,k}$ of every point $y_{j,k}$ (where $k = 0,\ldots,N_j$):

$$J_i^{j,k} = -a_i^j \frac{dc_i^{j,k}}{dx} + c_i^{j,k+\frac{1}{2}} \left(b_i^j E^{j,k} + \sum_{l=1}^{r} g_l^j \frac{dc_l^{j,k}}{dx} - \sum_{l=1}^{r} \chi_l^j c_l^{j,k} E^{j,k} + \sum_{l=1}^{r} \overrightarrow{\gamma_l^j} c_l^{j,N+1} - \sum_{l=1}^{r} \overleftarrow{\gamma_l^j} c_l^{j+1,0} \right). \quad (47)$$

The concentration at $x_{j,k}$ is a weighted linear combination of neighbouring concentrations:

$$c_i^{j,k+\frac{1}{2}} \approx (h_{j,k} c_i^{j,k} + h_{j,k-1} c_i^{j,k+1}) / (h_{j,k-1} + h_{j,k}). \quad (48)$$

The space derivative of the concentration at $x_{j,k}$ was approximated by a three-point, non-uniform finite difference:

$$\frac{dc_i^{j,k}}{dx} = 2 \frac{h_{j,k-1}^2 c_i^{j,k+1} - h_{j,k}^2 c_i^{j,k} + (h_{j,k} - h_{j,k-1})(h_{j,k} c_i^{j,k} + h_{j,k-1} c_i^{j,k+1})}{h_{j,k-1} h_{j,k} (h_{j,k-1} + h_{j,k})}. \quad (49)$$

Discretized electrical potential of each point in space, as well as overall potential in the system, can be expressed as:

$$\begin{aligned} \varphi^{j,k} &= -\sum_{g=1}^{k} \left(\frac{1}{2} (E^{j,g} + E^{j,g-1}) h_{j,g-1} \right), \\ \Delta\varphi &= \sum_{j=1}^{n} \varphi^{j,N_j} = -\sum_{j=1}^{n} \sum_{g=1}^{N_j} \left(\frac{1}{2} (E^{j,g} + E^{j,g-1}) h_{j,g-1} \right). \end{aligned} \quad (50)$$

In the multi-layer-model, the boundary points $x_{j,0}$, x_{j,N_j}, $y_{j,0}$, y_{j,N_j+1} are the points which have the surrounding in two layers. The first points of each boundary ($x_{j,0}$ and $y_{j,0}$) have the same value of space as the last points of previous layer (x_{j-1,N_j} and y_{j-1,N_j+1}), but different values of concentration and electrical field:

$$\begin{aligned} & x_{j,0} = y_{j,0} = x_{j-1,N_j} = y_{j-1,N_j+1}, \\ & c_i^{j,0} \neq c_i^{j-1,N_j+1}, \quad E^{j,0} \neq E^{j-1,N_j}, \quad J_i^{j,0} \neq J_i^{j-1,N_j}. \end{aligned} \quad (51)$$

The unconditionally consistent space discretization presented above is one order of approximation higher than used by Brumleve and Buck [81] (check publication III, for the detailed calculations of Local Truncation Error). The resulting system of non-linear ordinary differential equations (Cauchy problem) can be solved using one of the numerical integrators presented in the following chapter.

3.1.3. Integrator

The above discretization leads to the system of ordinary differential equations (ODEs) in time variable. Due to the stiff nature of these ODEs, a special integrator is needed. The source of the stiffness is connected with the method of lines which tends to produce this phenomenon for the diffusion terms [23].

Software presented in this thesis uses class StiffIntegratorT, an implicit integrator based on the procedure RADAU5, which has been implemented in C++ by B. Ashby. Source of this class is an object oriented interpretation of the procedure, written originally in Fortran by E. Hairer and G. Wanner [106].

StiffIntegratorT solves the vector $f_l(t)$, when derivative $\frac{df_l}{dt}$ is known and provided as a function. In the multi-layer model a three-dimensional array: $\left\{c_i^{j,k}, E^{j,k}\right\}(t)$, where $\frac{dc_i^{j,k}}{dt}$ and $\frac{dE^{j,k}}{dt}$ are known from equations 46-49, is transformed to a vector $f_l(t)$ and solved. Details concerning transformation of an array into a vector can be found in [98]

The comparison between various integrators, i.e. RADAU5 [106], RODAS [107], and SOULEX [106] can be found in publication III. The first two of them are based on the special types of implicit Runge-Kutta methods and the third is based on the extrapolation applied to linearly implicit Euler method. Good agreement of the results is obtained.

The integrator's time performance for typical electrodiffusion problems shows that none of them is the best for all cases, as the performance may strongly depend on specific values of physical parameters, e.g. boundary concentrations or heterogeneous rate constants.

3.2. Liquid Junction Potential

In the classical reference electrodes, an additional electrolyte solution called salt bridge is interposed between the external reference electrolyte and the sample in order to inhibit the interactions of these two solutions. The liquid junction between the salt bridge and the sample is usually established within a porous diaphragm or defined by a streaming boundary. Since the liquid junction represents the interface where one electrolyte diffuses into another, it is the origin of an electrical potential difference contributing to the overall potential of the cell [2].

The concept of the junction potentials formed over a "*watery contact zone*" was first developed over a century ago by Nernst [108] and Planck [109]. Most recent review concerning the analysis and simulation of liquid junction potentials can be found in the paper of Dickinson, Freitag and Compton [110].

Liquid junction may be described as an imaginary barrier separating two different bathing solutions of electrolytes connected by the means of a porous plug [111]. It has a limited width and possesses the same physical characteristics as water. This "classical" approach, derived by Planck [67,109] and defined by Guggenheim [112] as "constrained" liquid junction, has been widely used (e.g. in [35,44,81,83,96,113,114,115]). An alternative approach, known as "free" liquid junction, instead of the unphysical barrier describes a dynamically relaxing junction of two liquids in which a diffuse layer continues to expand in a linear semi-infinite space. The "free" junction was first presented in the work of Hafemann [116] and its dynamics were discussed in more detail in the recent review [110].

In publication III, the time-dependent potential response of liquid junction was investigated. Analysis of such response is important for the practical applications, due to the development of fully automatic methods of analytical potentiometry, where short readout times may provoke instability of the liquid-junction potential, especially in a case of clinical electrolyte analysers [117].

Evolution of the electric potential can be systematically divided into four stages:

1) Initially, the deviation from electroneutrality and consequently change of the electric field profiles occurs close to the contact of the solutions, until the value of electric field reaches the maximum.

2) The deviation from electroneutrality and consequently the change of the electric field propagate through the system, while their maximum values decrease. During this stage, the position of maximum deviation from electroneutrality and maximum electric field moves

away from the center of the system (the initial junction location). In this stage the potential is convergent to a certain value, which corresponds to the value of steady state potential in the "free" liquid junction approach. In this approach, the electric field relaxes back to zero at infinite time.

3) The third stage begins when the deviation from electroneutrality and consequently the change of the electric field reaches the boundary. The values of maximum deviation from electroneutrality close to the boundary and the electric field at the boundary are increasing during this stage.

4) When they reach their maximum values, the steady state (fourth stage) is reached. The fluxes are constant across the system and no further changes of concentration or electric field occur.

In publication III, the steady state values of a "constrained" liquid junction potential obtained using the NPP model in the form described in this thesis at "infinite time" are also compared with the published values according to Planck, Henderson, and the evolutional (NPP based) method described by Sokalski et al.

Planck in his "classical" approach [67,109] considered monovalent ions and assumed the electroneutrality. Using Dirichlet boundary conditions, he derived the formula for a steady-state diffusion potential. The Planck solution does not generally yield the diffusion potential explicitly but has to be evaluated by iterative methods. His original derivation is quite complicated. Much simpler derivation and without the restriction to monovalent ions, was offered by Morf [118].

Henderson [119, 120], based on the assumption that concentrations at a steady state in the membrane are linear in space, derived thermodynamically the well-known equation for a membrane potential:

$$\varphi = -\int_0^d E(x)dx = -\frac{RT}{F}\frac{\sum_{i=1}^{r} z_i D_i (c_i(d) - c_i(0))}{\sum_{i=1}^{r} z_i^2 D_i (c_i(d) - c_i(0))} \ln\left(\frac{\sum_{i=1}^{r} z_i^2 D_i c_i(d)}{\sum_{i=1}^{r} z_i^2 D_i c_i(0)}\right). \quad (52)$$

In Sokalski-Lewenstam method [35,44], the liquid junction potential is calculated as an asymptotic steady-state solution of time-dependent NPP problem assuming "infinite" heterogeneous rate constants. The implicit Euler time discretization scheme and conditionally consistent space discretization followed the approach of Brumleve and Buck [81].

The above methods, described in more detail, as well as the diffusion potential calculated using these methods for different solutions and concentrations can be found in publication III.

Lingane in his work [121] presented a classification, dividing the liquid junction solutions into three types:

- type 1 – junction of two solutions of common phase but different concentrations,
- type 2 – junction of two solutions of different phase but common concentrations,
- type 3 – all other liquid junctions.

For the liquid junctions of type 1 and 2, the Planck's formula reduces to the form equivalent to the Henderson equation. Consequently, the comparison in publication III shows that for type 1 liquid junction (the KCl/KCl case), Planck and Henderson equations give the same values. In addition, the results obtained with methods using NPP model agree with these values. Furthermore, calculated concentration profiles show the linearity.

For Lingane's type 3 liquid junction (the KCl/HCl case) the results calculated using the NPP model are closer to the Planck solution than the ones obtained using the Henderson equation. This results from the fact that for ions having appreciably different diffusion coefficients the resulting steady-state concentration profiles are not linear, and this is contrary to Henderson's assumption. The Henderson equation is inexact for liquid junctions of type 2 and 3, as it was proven already in 1970 [122] using asymptotic analysis.

In their recent work, Ward et al. [123] presented more detailed analysis of type 3 "free" liquid junction. The time-dependent potential response of type 3 junction is analogical to the response of the junctions' type 1 and 2. They observed that the AX|BY system with different diffusion coefficients ($D_{A^+} \neq D_{X^-}$ and $D_{B^+} \neq D_{Y^-}$) has a tendency to create so called multilayer liquid junction. In this type of junction, instead of one maximum of electric field occurring in the vicinity of the initial junction location (as for the other liquid junctions), one local minimum surrounded by two satellite maxima is observed. In order to obtain multilayer liquid junction for AX|BY system, one of three following conditions has to be met: $D_{A^+} < D_{B^+} \leq D_{X^-} < D_{Y^-}$ or $D_{A^+} < D_{X^-} \leq D_{B^+} < D_{Y^-}$ or $D_{X^-} < D_{Y^-} \leq D_{A^+} < D_{B^+}$.

The reference electrode systems have thus far been interpreted almost exclusively by the Henderson equation [132]. The use of NPP brings the modelling of liquid junction potentials closer to physical relevance and allows the consideration of finite rate constants

and multilayer composition of the bridge with varying ion mobilities and resulting overall reference electrode potential response. One may stipulate that this method will be a good tool for analyzing transient potentials on the salt bridge in the reference electrodes, which may be source of error in certain practical applications [44] (e.g. sluggish response of the reference electrodes with a constrained liquid junction in clinical analyzers [117,124,125]).

All above discussions were devoted to the junction of two solutions based on a single solvent (i.e. water). Similar systems – i.e. "free" junctions of two solutions based on different immiscible solvents were very recently studied using the NPP model by Zhurov et al. [126,127]. Between such two solutions, an interface is formed and the ion transfer reactions take place as ions are partitioning into one particular solvent for energetic stabilization.

In such systems the time-dependent potential response can be divided into three characteristic stages. For the short times, when the changes in the system occur only in a boundary layer (within the Debye-Length range from the interface), we observe stage 1 directed by thermodynamic drive for the ions to partition between two solutions. In stage 2, the changes in the system extend beyond the boundary layer the migration term becomes significant and the system starts to restore electroneutrality. Stage 3 is dominated by the elimination of charge separation in order to fully restore the electroneutrality outside boundary layer.

3.3. Lower Detection Limit - Comparison of the Models

The detection limit is one of the constitutive parameters of ISE. The definition of the detection limit of ISEs according to the IUPAC recommendations (cross section of the two extrapolated linear segments of the calibration curve [128]) takes into account only the flattening of the response. In this thesis, the definition presented in [57] is used, which takes into account also the increase of the slope. Detection limit is defined as a bulk concentration at which the measured potential begins to deviate by $RT / z_i F \ln 2$ in either direction from the Nernstian value.

Typically, the detection limit of ISE lies in a micromolar range [14,15]. The detection limit of ISEs can be engineered to vary by several orders of magnitude depending on the inner solution concentrations or the time of measurement. It can be lowered, even down to a picomolar range, by using inner solutions whose concentrations of analyte ions are kept at the low level as was shown by Sokalski et al. [58]. This prevents the preferred ions from leaching from the inner solution, through the membrane to the diffusion layer. Such a leaching process (the effect of transmembrane fluxes) causes the analyte ion concentration at the phase boundary to be significantly higher than in the sample bulk [129,130].

The NPP system allows the electric potential and concentrations as functions of space and time to be found. It is valid also in the field of ISEs, even though they are generally used in the steady state. The "classical" models are derived under steady state assumption, but they are based on further simplifications as it was presented in previous chapters. The steady state ISE potential can be found as an asymptotic value of the time-dependent evolving potential based on NPP model. The NPP system, integrated up to the time when steady state is reached, gives better results for the modelling of ISE potential response [3,131].

Publication I presents a critical comparison of three different models describing the behaviour of ISEs (both for transient and steady-state response), namely Steady State Diffusion Model (SDM) [57], described in chapter 2.2., Time Dependent Exchange-Coextraction Model (TDM-EC), described in chapter 2.3., and multi-layer NPP model (chapter 3.1.). This comparison can exemplify and clarify the basic merits and weaknesses of different approaches.

The PBM purposely ignores the diffusion potential (assuming it to be negligibly small or constant) and only the boundary potential is considered. This contradicts the recent findings demonstrating the improvements of the detection limit due to the manipulation

of transmembrane fluxes [57,58,132,133]. The necessity of including diffusion potential in the interpretation of ISEs and their response was recently emphasised in the works of Mikhelson and Lewenstam [43,134,135]. The NPP model not only allows us to calculate the diffusion potential alone (see chapter 3.2.) but also allows us to abandon the previously necessary split of membrane potential into boundary and diffusion potentials.

The comparison in publication I was strictly limited to the models which are directly relevant to the description of lower detection limit phenomenon [58]. As this phenomenon is an effect of the presence of the diffusion layer, simple models (i.e. PBM – chapter 2.1.) cannot be applied.

The use of NPP for the description of the detection limit phenomenon shows when the simplifications are justified. In the case of steady-state calculations and for monovalent ions the tendencies shown by the SDM and TDM-EC model were confirmed with NPP simulations. The agreement between these three models is very good.

For lower concentrations of the preferred ion in the sample solution especially, the influence of diffusion layer is crucial. The concentration of ion near the membrane boundary is different than inside the bulk as it is shown in Fig. 4. The model reduced to one layer is thus insufficient and the correct description of detection limit can only be obtained by using the multi-layer model, which takes the effects of diffusion layer into consideration.

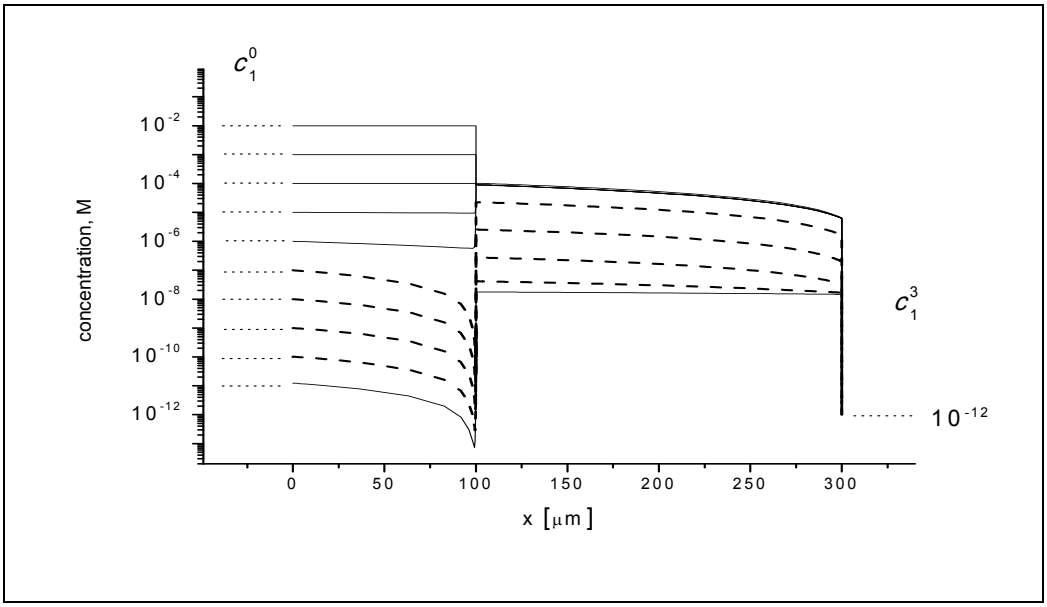

Figure 4. *Steady state concentration profiles of main ion. Concentration of the preferred ion in the sample changed in the range* $10^{-11} \div 10^{-2} M$.

The influence of various ISE parameters on the detection limit of ISE, namely: concentrations of discriminated ion in the sample and in the inner solution, values of exchange constant and coextraction constant, total concentration of the anionic sites in the membrane, as well as the diffusion coefficients, has been studied in publication I.

Decreasing the concentration of the preferred ion in the inner solution, or the coextraction constant (anion lipophilicity), improves the detection limit by several orders of magnitude towards the picomolar range, as was already presented in [57]. After reaching an optimal value (for which the concentration of preferred ion at the membrane boundary becomes equal to the one in the bulk) the detection limit worsens with a further decrease of one of these two parameters and a super-Nernstian, "titration-like" response is observed (concentration of preferred ion at the boundary becomes lower than in the bulk). The influence of the concentration of the preferred ion on the potentiometric response of ISE is illustrated in publication I (Fig. 4).

In addition, the decrease of the parameters such as the concentration of the discriminated ion in the inner solution, the ionic site concentration or the diffusion parameter (representing the influence of diffusion coefficients in both layers and their thicknesses, i.e $DP = D_i^2 d_1 / D_i^1 d_2$), leads to a lower detection limit for all electrodes. In order to design an electrode with the lowest possible detection limit, all values of the parameters listed above should also be as low as possible.

The exchange constant and the concentration of the discriminated ion in the bulk of the solution have little influence on electrodes with a nearly optimal concentration of preferred ion in the inner solution. Neither do they significantly affect the level of the super-Nernstian plateau for electrodes which show this type of response.

Also the transient-state response of ISE has been investigated. The NPP simulations presented in publication I, show the influence of time on the detection limits. For the electrodes in which the outward flux of the preferred ion is either under-compensated or ideally compensated, the detection limit decreases with the increase of time. For electrodes in which the outward flux of the preferred ion is over-compensated, the detection limit decreases with the increase of time, reaches an optimum and then worsens again because of the super-Nernstian response, as it is shown in publication I (Fig. 1). For transient-state

measurements, much lower (subnanomolar) detection limits can be achieved than for steady-state measurements.

The difference between the transient-state predictions of TDM-EC and NPP is significant. TDM-EC predicts that the steady-state is reached almost immediately. The NPP predicts that the system will obtain steady-state more slowly. This example nicely illustrates the role of the potential formed inside the membrane and the effects of the migration process on the ISE signal evolution. The electric field inside the membrane retards the transport of the faster moving ion, and consequently slows down the process of reaching steady-state.

This is a definite proof that the more general NPP model quantitatively reflects the important processes that arbitrary are not considered by simpler models in the cases of non-equilibrium response and can be of a better use for the description of fast analysis, e.g. with automated clinical analysers. NPP is clearly superior to earlier approaches to describe the ISE potential by modifications of Nikolsky-Eisenman equation (forgetting that this equation is already an empirical postulate), e.g. by applying Fick's law for ions and assuming that they are uncharged [136] or by guessing a time function [49].

The NPP model is by far the most general of the models discussed in this thesis. Using NPP makes it possible to take into account bigger number of components, polyvalent ions, and transient-state potential measurements. Therefore, the NPP model can be used for the description of a much wider range of phenomena concerning ISEs than PBMs or the DLMs. It is also a tool to justify the use of simpler models in certain situations.

3.4. Ion-Exchanger and Neutral-Carrier Membranes

Membranes with fixed, electrically charged ion-exchange sites were developed in the 1920s [137] and 1930s [138]. Such membranes are easily permeable for counterions (ions attracted by ion-exchange sites) but poorly permeable for oppositely charged ions. The theory of ion-transport through such membranes was pioneered by Beutner [139], Teorell [70,140], Meyer and Sievers [141] and later generalized by Schlögl [68] and Helfferich [69].

The classical Teorell-Meyer-Sievers theory assumes the ionic sites to be "fixed", i.e. trapped and evenly distributed within the membrane phase. The calculations using the NPP model clearly shows that the even distribution of ion-exchanger in the membrane phase is not a correct assumption. The value of the concentration of the ionic sites near the boundary can significantly vary from the one in the bulk of the membrane (see Fig. 5d in publication I).

Among the various DLMs used for the description of ion-exchanger membranes, it is worth to mention the Jyo-Ishibashi model (shown in [2]), which describes the response of ion-exchanger ISEs subjected to a solution of strongly preferred ion ("Hulanicki effect"). Its later modification [142] allows the description of the response of ion-exchanger electrodes at low-concentration levels.

The NPP simulations of such systems are common and have been described in numerous papers, among them in publications I, II and V. The apparent selectivity of this type of ISEs was investigated using the NPP model by Lingenfelter et al. [88].

Many of the ISEs used nowadays for the industrial applications contain the neutral ionophores [3]. These lipophilic molecules, of rather small relative molar mass, are capable to selectively complex certain ions, solubilising them in organic phase and transporting them across the membrane.

The effect of naturally occurring neutral-carrier antibiotics in biologically neutral systems was discovered in 1964 [143]. The role of neutral carriers as highly selective complexing agents was recognised three years later by Štefanac and Simon [144]. The striking discrimination between Na^+ and K^+, shown by valinomycin and the macrotetrolides, led them to the pioneering idea of utilising such neutral ionophores as ion-selective components in membrane-based electrodes. Although the first specimens of neutral-carrier electrodes were considered to be "exotic systems" [145], nowadays they

are very widely applicable. The outstanding selectivities of these electrodes opened attractive applications in analytical and clinical chemistry, e.g. measurements of ion activities in blood serum or whole blood [146].

The response of the ionophore based sensors was investigated using PBM in the work of Ngele et al. [147] and theoretically compared with the response of ion-exchanger ISEs.

The NPP model presented in chapter 3.1., as well as other solutions NPP systems analysed in the literature so far, did not include the information about the ligands and complexes they are forming (for the simplicity of the description). The description of the neutral-carrier membranes using the NPP model was therefore realized using the assumption that the ions are fully associated by the ligand (like e.g. in [88,148]).

In order to include the full information about the formation of complexes in the NPP model, the mass conservation law (eq. 25) was accompanied with the reaction term, which for the reactions $I^+ + L \rightleftarrows IL^+$ and $J^+ + L \rightleftarrows JL^+$, takes the form:

$$
\begin{aligned}
\frac{\partial c^2_{I^+}(x,t)}{\partial t} &= -\frac{\partial J^2_{I^+}(x,t)}{\partial x} + k_{I,dis} c^2_{IL^+}(x,t) - k_{I,as} c^2_{I^+}(x,t) c^2_L(x,t) \\
\frac{\partial c^2_{J^+}(x,t)}{\partial t} &= -\frac{\partial J^2_{J^+}(x,t)}{\partial x} + k_{J,dis} c^2_{JL^+}(x,t) - k_{J,as} c^2_{J^+}(x,t) c^2_L(x,t) \\
\frac{\partial c^2_L(x,t)}{\partial t} &= -\frac{\partial J^2_L(x,t)}{\partial x} + k_{I,dis} c^2_{IL^+}(x,t) - k_{I,as} c^2_{I^+}(x,t) c^2_L(x,t) + \\
&\quad + k_{J,dis} c^2_{JL^+}(x,t) - k_{J,as} c^2_{J^+}(x,t) c^2_L(x,t) \\
\frac{\partial c^2_{IL^+}(x,t)}{\partial t} &= -\frac{\partial J^2_{IL^+}(x,t)}{\partial x} - k_{I,dis} c^2_{IL^+}(x,t) + k_{I,as} c^2_{I^+}(x,t) c^2_L(x,t) \\
\frac{\partial c^2_{JL^+}(x,t)}{\partial t} &= -\frac{\partial J^2_{JL^+}(x,t)}{\partial x} - k_{J,dis} c^2_{JL^+}(x,t) + k_{J,as} c^2_{J^+}(x,t) c^2_L(x,t)
\end{aligned}
\tag{53}
$$

where $k_{I,dis}$ and $k_{I,as}$ represents dissociation rate constant and association rate constant for the IL^+ complex, while $k_{J,dis}$ and $k_{J,as}$ represents dissociation and association rate constant for the JL^+ complex. I^+ and J^+ represent preferred and discriminated ion respectively and L represents the ligand. Ligand can form the complexes with both preferred and discriminated ion, but the rate constant for the formation of JL^+ complex is much lower than for the formation of IL^+ complex.

In this thesis, the first full theoretical description of neutral carrier ISEs was presented and the discussion about the influence of various parameters on detection limit was performed.

.

As it is presented here, ligand creating the complexes with the preferred ion influences the potential response of ISE. Inclusion of the reaction into the model allows to lower the detection limit. Reaction always influences the time-dependent response of ISE, but only in the case of very short time of measurement or low concentration of analyte in the sample it can change the value of the resulting potential.

Fig. 5 shows the calibration curves, both considering the reactions between the preferred and discriminated ion with the ligand ($I^+ + L \rightleftarrows IL^+$ and $J^+ + L \rightleftarrows JL^+$ for monovalent ions and $I^{2+} + L \rightleftarrows IL^{2+}$ and $J^{2+} + L \rightleftarrows JL^{2+}$) for divalent ones and without taking these processes into consideration. The results presented here show clearly that in both considered cases, the creation of the complex (IL^+, JL^+ and IL^{2+}, JL^{2+} respectively) lowers the detection limit of ISE by two orders of magnitude. The reaction does not influence the slopes of the calibration curves, that equal $58\,mV$ and $29\,mV$, respectively.

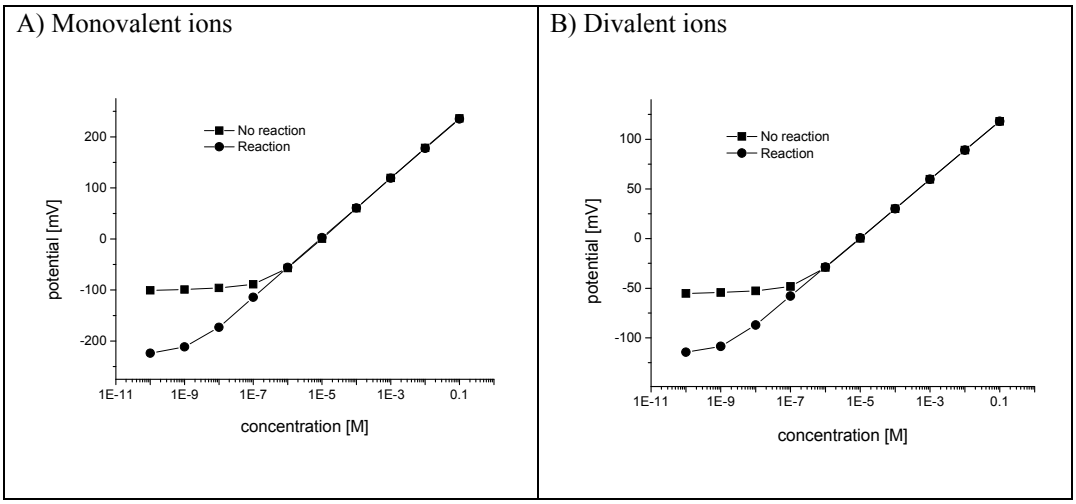

Figure 5. *Calibration curves of ISEs obtained using the NPP model with and without the reaction term.*

Fig. 6 shows concentration profiles of the species (after $t_{END} = 300\,s$ of measurement of a particular point) for calibration curve points where sample concentration of preferred monovalent ion equals $c^0_{I^+} = 10^{-1}\,mol \cdot dm^{-3}$ and $c^0_{I^+} = 10^{-10}\,mol \cdot dm^{-3}$ respectively, both when the reaction is and is not considered. The results show that for all chosen concentration points, creation of complexes not only decreases the concentration of free

preferred ion I^+ in the membrane, but also reduces the concentration of discriminated ion in the membrane, because the ratio of the concentrations is kept constant and depends on the ratio of heterogeneous rate constants. Furthermore, the chemical reaction decreases the effect of preferred ion leaching from the internal solution. This effect causes the preferred ion concentration at the phase boundary to be significantly higher than in the sample bulk (see Fig. 6c,d) and is one of the primary causes of worsening of the detection limit [129,130]. The complexing reaction causes the concentration of free preferred ion in the membrane to decrease, preventing the effect of leaching, which reduces the transmembrane fluxes and consequently leads to the improvement of the detection limit (see chapter 3.3.).

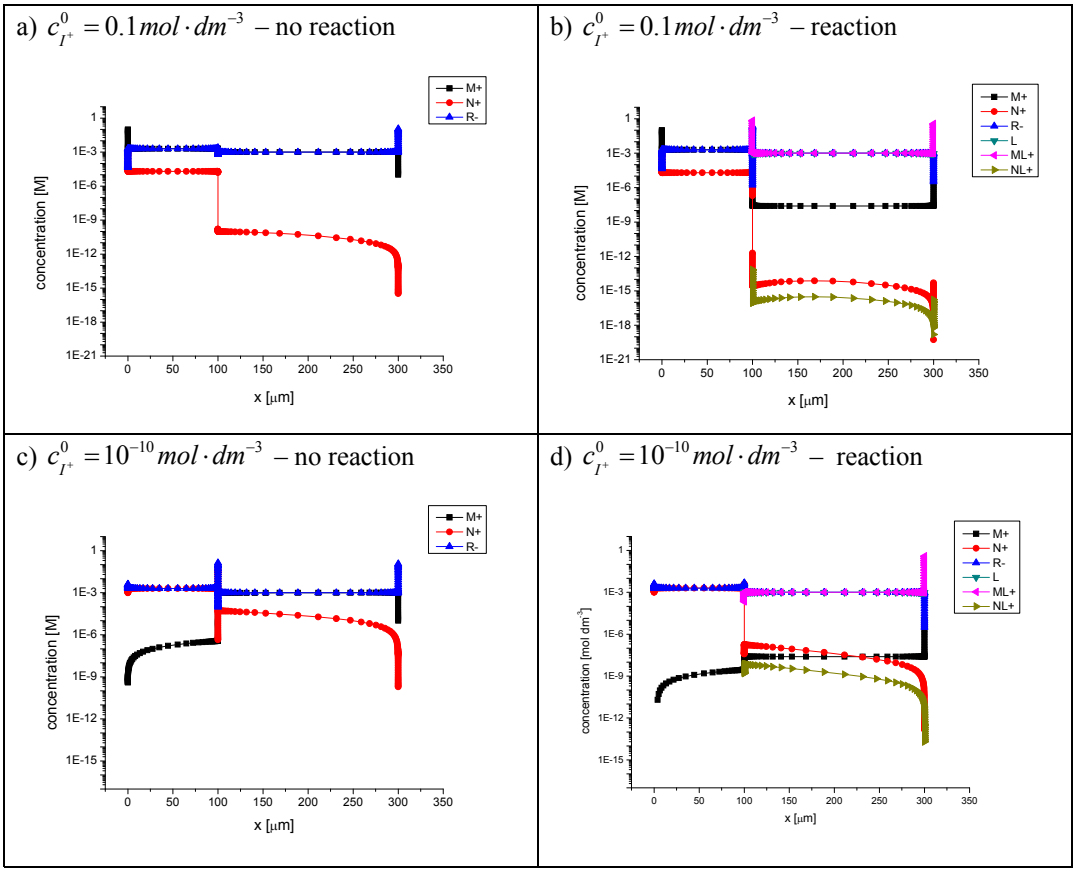

Figure 6. *Concentration profiles, obtained using the NPP model with and without the reaction term. System consisting of 100μm diffusion layer and 200μm membrane.*

Moreover for the monovalent ions case, we perform the calibrations, changing the value of association rate constant $k_{I,as}$ in the range $1 \div 10^6$, which corresponds

to the change of stability constant β_1 in the same range. As shown on Fig. 7a, the higher is the stability constant, the lower is the detection limit.

In a typical membrane, the initial concentration of ligand L is twice as high as the concentration of anionic sites R^-. In our simulations (for monovalent ions case) we changed the concentration of ligand in the range $2 \cdot 10^{-4} \div 10^{-2}\, mol \cdot dm^{-3}$. Results presented at Fig. 7b show, that the increase of the concentration until reaching twice the concentration of the anionic sites ($c_L^2 = 2 \cdot c_{R^-}^2 = 2 \cdot 10^{-3}\, mol \cdot dm^{-3}$) lowers the detection limit significantly. Further increase of the concentration of ligand above this value does not improve the detection limit. These results correspond very well to the empirical observations.

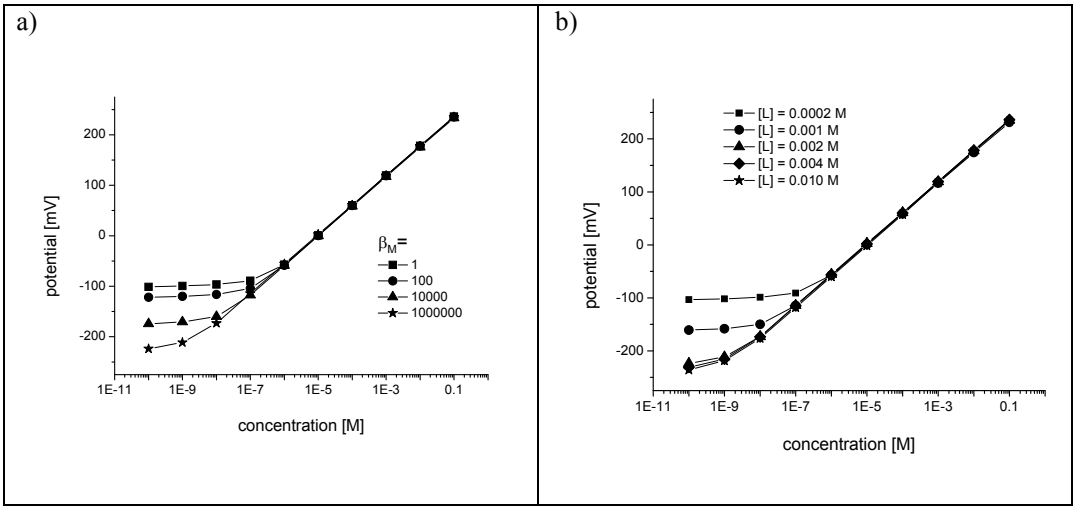

Figure 7. *a) Calibration curves, obtained using the NPP model with the reaction term with various stability constants. b) Relationship between selectivity coefficient and stability constant.*

Ligand creating the complexes with the preferred ion, influences the potential response of ISE. For both monovalent and divalent ions including the reaction into the model, allows to lower the detection limit by two orders of magnitude. Reaction always influences the time-dependent response of ISE, but only in the case of very short time of measurement or low concentration of analyte in the sample it can change the value of the resulting potential.

Including the effects of ionophore and the complexing reactions makes the modelling more relevant (i.e. closer to real cases) and allows better description of neutral carrier ISEs.

3.5. Solid-Contact ISE – Comparison with Experiment

In all examples presented in the previous chapters, the ISEs with the inner filling solution were investigated. The recent trend in ISEs research involves the replacement of the inner filling solution by an intermediate layer between electrically conducting substrate and the solvent polymeric membrane. Elimination of the internal filling solution from conventional ISEs, can reduce trans-membrane ion fluxes to the sample solution causing the improvement of the detection limit and results in creation of more durable and easier to miniaturize solid-contact ISEs.

Research and development of such ISEs had started in 1970s, with the invention of the coated-wire electrode (CWE) [149]. In this ISE the blocked interface, formed between the purely electronic conductor (i.e. metal) and purely ionic conductor (i.e. ion-selective membrane), results in poor potential stability. In order to improve the potential stability requires a usage of ion-to-electron transducer (showing mixed electronic and ionic conductivity) between electronic conductor and ion-selective membrane [150].

Many various materials are used as ion-to-electron transducers; among them Ag/AgCl [151], Ag/AgCl/hydrogel [152], redox-active self-assembled monolayers [153,154], carbon-based composites [155,156,157]. Among the electroactive materials available today the conjugated polymers (CPs) are widely used [158,159,160,161,162,163] and becoming one of the most promising ion-to-electron transducers [164,165]. Owing to their mixed conductivity, CPs serve as the elements that unblock the faradaic charge transfer at the contact interfaces and thus adequately act as ion-to-electron transducers. In one of the recent reviews, Bobacka et al. [3] describe in detail the usage of polypyrroles, polythiophenes and polyanilines in determination of both inorganic and organic ions.

One of very interesting applications of conducting polymers are single-piece electrodes [166], where the polymer is dissolved in ion-selective membrane. This type of electrode is out of the scope of this thesis. Conducting polymers make it possible to fabricate e.g. all plastic ISE [167], and pH nanoelectrodes [168].

Modelling of the ion-selective electrodes with the CP used as ion-to-electron transducer was first presented in publication IV. The ISE with conducting polymer film made of polybenzopyrene doped with Eriochrome Black T (EbT) and PVC-based membrane containing lead ionophore IV (together serving as a lead-sensitive film), was investigated experimentally and using the NPP model (chapter 3.1.). The complexity of presented ISE

requires advance modelling, and makes the usage of the simple models presented in chapters 2.1. - 2.3. impossible.

In the NPP model, such ISE is represented by the three-phase (diffusion layer, membrane, CP) system with the electro-diffusion of five species: preferred ion - Pb^{2+}, discriminated ion Na^{+}, ion of the opposite charge NO_3^{-}, ionic site R^{-} representing tetrakis(4-fluorophenyl)-borate $TFPB^{-}$ and various bivalent impurities X^{2+}. As the stability constant for a complex of Pb^{2+} and lead ionophore IV is high, we used the assumption that the ions are fully complexed by the ligand (no reaction term, like e.g. in [88]). The preparation of ISE with CP has to be followed by the process of conditioning in the solution of preferred ion. The ISE was conditioned for 20 minutes and the calibration curve was measured. These two steps were repeated twice, which was accordingly modelled using NPP.

The results confirm that during the process of conditioning the preferred ion is transported in through the ion-selective membrane and accumulated in the layer of CP. The calibration curve obtained after first conditioning has a super-Nernstian response similar to the classical ISE with very low value of concentration of preferred ion in the inner solution (see chapter 3.3.). The calibration curves obtained after second and third conditioning have the Nernstian response and the value of detection limit after the second conditioning is lower than after the third. These responses are analogical to the responses of classical ISEs, with optimal and high value of concentration of preferred ion in inner solution, respectively (see chapter 3.3.). The NPP model confirms qualitatively the experimental results (process of enriching the polymer with the preferred ion leads to the changes in the detection limit and slope of the electrode over time). Moreover, the detection limits obtained in the experiments correspond well to the ones obtained from the simulations.

Publication IV, delivered the first consistent interpretation of the responses of solid contact ion-selective electrodes with conducting polymer used as an intermediate layer. The qualitative agreement (shape of calibration curves and value of detection limit) is reached. The quantitative agreement isn't achieved, due to the fact that the parameters of the system are unknown and the values used in numerical simulations are estimated. The qualitative agreement can be obtained by using stochastic methods to search for optimal parameters, which leads to another possible application of NPP-HGS method (chapter 3.7.). Including the reaction term (chapter 3.4.) of complexation reactions in the CP can also lead to more realistic description of all-solid-state ISEs.

3.6. Electrochemical Impedance Spectroscopy

The range of applications of the Nernst-Planck-Poisson model is wider than the description of processes occurring in potentiometry. In publications III and VI, the application of NPP for the description of Electrochemical Impedance Spectroscopy (EIS) was presented.

EIS is a very powerful tool for the analysis of various complex electrochemical systems [169]. It allows the separation and characterization of individual kinetic processes. It is a technique for the versatile characterisation of interfacial processes and structures as well as other material properties, based on their electrochemical responses. It can be used (among other applications) for the analysis of electrode kinetics, double-layer, batteries, corrosion mechanisms and the membranes in analytical chemistry [170].

Typically, several cell elements, such as e.g. electrode double layer capacitance, electrode kinetics, diffusion layer and solution resistance, contribute to the system's impedance spectrum.

One of the commonly used techniques in the interpretation of impedance spectra is building an equivalent circuit model which corresponds to the electrochemical system [169]. Such circuits, constructed from simple passive elements (i.e. resistors, capacitors, etc.), simply reproduce the properties and represent incomplete analysis of the data [171,172]. There are several problems connected to this approach, e.g. the equivalent circuits may not be unique and it is not always possible to describe complex electrochemical behaviour with such circuit elements.

Alternatively to the use of equivalent circuits, the physical modelling can be used to interpret the impedance spectra. The first theoretical description of the diffusional impedance was developed by Warburg [173,174]. In 1903, Krüger in his work [175] merged Warburg's theory with the Helmholz double layer concept providing more complete understanding of electrochemical polarisation. Three decades later, Jaffé in his theoretical treatment of cells with blocking interfaces [176] included the effects of space charge, migration terms and ion recombination. His theory was later extended by Chang and Jaffé [101] to include electrode the discharge of current carriers. Tribollet et al. [177], using electroneutrality assumption, derived an analytical solution of diffusion-migration equations coupled with the description of electrochemical reactions occurring at the surface of metal electrode. Another similar approach, also allowing the calculation of complex impedance of solution | metal system, was presented by Dan et.al [178].

The first application of NPP model for interpreting the impedance spectra has been developed by Macdonald [179,180]. Unfortunately, even for very idealised cases considered in his work, complex algebraic equations were obtained. Interesting application of NPP, simplified by the use of electroneutrality, steady state and arbitrary summation was presented recently [181].

The more fundamental and universal approach presented by Brumleve and Buck [81] and followed in this thesis, refers directly to the physical processes in the system, relating the impedance spectra to the physical parameters and is free from approximate assumptions. It is based on the numerical solution of NPP model in which the current perturbation is treated as an input parameter and the impedance spectrum (calculated from the time-dependent electric potential) is calculated as an output. This approach allows calculation of the impedance spectra without approximate assumptions (like e.g. linear dependence of the potential) and directly relates them to the physicochemical parameters of the system.

Electrochemical impedance is usually measured by applying a time-dependent potential disturbance to an electrochemical cell and measuring the current through the cell. Conversely, a small current perturbation can be applied and the resulting potential response analyzed. If a sinusoidal or step-function current excitation signal is applied, the response to this signal is an electric potential, which evolves in time and contains the excitation frequency and its harmonics. These excitation-response characteristics can be compactly and clearly presented in the graphical form of the so called impedance spectrum on the complex plane.

In EIS we measure an electrochemical cell's complex impedance over a wide range of AC frequencies (sinusoidal excitation signal) or by applying only one step-function perturbation to the system (first at zero total current density – open-circuit, then with a constant non-zero total current density, as was done in [81]). The results obtained using the NPP model, presented in this thesis, with both sinusoidal and step-function perturbations show that these two methods are in very good agreement. Details for both methods as well as their comparison are presented in publication VI.

The typical Impedance spectrum of an ISE membrane consists of two or three arcs. First arc, at high-frequencies is related to the bulk properties of the membrane. In the terms of equivalent circuits, it can be interpreted as charging of the bulk capacitance, in parallel with the resistance [81, 181]. The second one at low frequencies corresponds to the effects of diffusion inside the membrane. At higher frequencies it exhibits the $\pi/4$ slope and at lower

frequencies semicircle – this type of response is characteristic for the Warburg impedance. If the interfacial kinetics is sufficiently fast (comparing to other processes limiting transport of ions), only these two arcs are predicted [181,182].

The size of these two arcs corresponds to the value of system impedance and increases with the increase of the membrane thickness [183]. The size of the arcs changes also gradually with the concentrations of the ions in the bathing solution, in the intermediate region between two boundary states. This intermediate region of concentrations is the region when the electrical potential is the effect of both ions (in the boundary states it depends only on the preferred or only on the discriminated one). The shift in the intermediate region (observed both in theory [96,183] and in the experiment [184]), is presented in publication III.

If the interfacial kinetics becomes sufficiently slow (e.g. by lowering the values of heterogeneous rate constants or the membrane width), the additional arc attributed to the interface impedance develops in the medium frequencies [81,99]. In the terms of equivalent circuits, it can be interpreted as charging of the double layer capacitance, through the surface resistances at both interfaces. When the kinetics becomes even slower, the medium-frequency arc starts to dominate. The behaviour of this arc is illustrated in [81], [96], [183] and publications III.

3.7. Hierarchical Genetic Strategy

Various parameters, such as concentrations in inner solution, layers thicknesses, diffusion coefficients, heterogeneous rate constants and time of measurement, determine the electrochemical response of the sensors. Finding optimal values of these parameters can have a crucial impact on the design of new electrodes. In order to find these optimal values, the “inverse problem” has to be formulated, namely the question "Which set of NPP parameters produces the desired response?” has to be asked. Formulation of the inverse problem in NPP modelling leads to obtaining the function with many optima (maxima and minima).

Problems with many optima can be efficiently solved using genetic algorithms [185,186]. The genetic algorithms are relatively new branch of science, but already found various applications in mechanics, automatics and biochemistry, especially in structural optimization and identification problems [187]. The idea they are based on comes from the surrounding nature, i.e. while looking for an optimal solution the algorithm is mimicking the evolutional mechanisms.

The main advantage of genetic algorithms is the possibility to achieve much lower computational complexity than the one of deterministic algorithms. The price that all stochastic algorithms pay for their low complexity is the lack of certainty to find the optimal solution. The main aim of evolutionary strategies is to improve their effectiveness, while keeping the complexity low.

In this type of algorithms, we formulate a problem with the solutions belonging to a defined environment (set of feasible solutions). The elements of this environment are called phenotypes. There is also a function, known as fitness function, assigned to this environment estimating the solutions. Algorithm works on populations (groups) of individuals. Each individual has its own genotype, which is a recipe to create a phenotype – the element of the environment. For each individual, it is possible to calculate the value of the fitness function, which can be understood as a level of adaptation of this individual.

The genetic algorithm can be described using the scheme presented in Fig. 8. During the initialisation of the algorithm, the starting population is chosen. The algorithm evaluates this population, i.e. calculates the fitness function for all individuals. If the stop condition is not achieved, the new population is created using the genetic operators and selection. The new population becomes a starting population for another run of the loop.

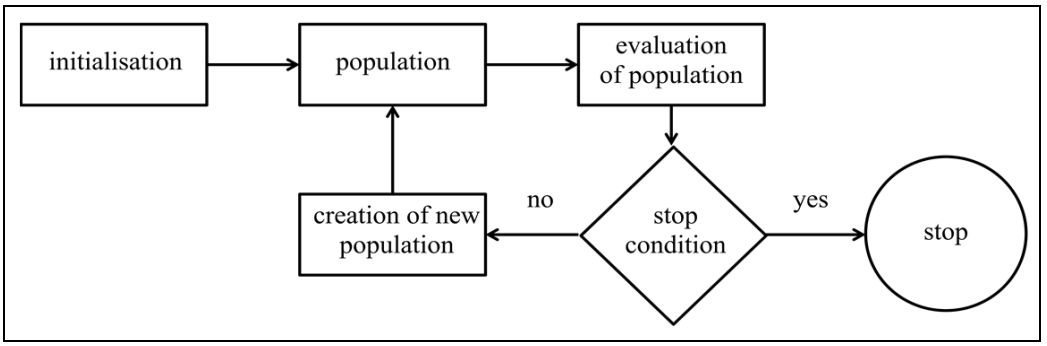

Figure 8. *Scheme of a simple Genetic Algorithm.*

The genetic operators are used to modify the genotypes of the individuals. We distinguish two genetic operators:

1) Mutation - generation of a new individual from the already existing one, by perturbation of its genotype. It allows the individual to move through the environment which allows random search in large areas.

2) Crossover - generation of a new individual from two already existing ones, by mixing their genotypes.

These two genotypes work together. One can either mutate the parent individuals and make a crossover or first make a crossover and mutate the child individual.

The selection is choosing the group of individuals from the population. It works randomly, based on the assumption that better adapted individuals have the bigger chance to "survive".

Based on the idea presented above many innovative solutions were developed. One group of such innovations are the multi-population algorithms. These algorithms are based on the concurrent search inside the optimization space by small populations developing parallely. Populations can exchange the genetic information and interfere in each other's development. Such strategies make the algorithm faster and the proper connections between the populations can significantly improve their efficiency.

Hierarchical Genetic Strategy (HGS) is one of the multi-population algorithms. It was introduced by Kołodziej et al. in the beginning of this century [188,189]. The main idea behind the HGS is a parallel transformation of co-dependent evolutionary processes. The algorithm evolves, creating the structures with different encodings (functions transferring sets of genotypes into sets of phenotypes).

Main structures in this strategy are branches, which create a tree with the established amount of levels. Encoding and the genetic operators are set in the way that the search

on the lower levels (closer to the root) are characterised with more chaotic search of solutions. On these levels the areas where the potential extrema can be found are established. When such areas are found, the process on the higher level starts to search the solution in these particular areas and their surroundings.

Each branch works in the following way: it is initiated (randomly in case of a population in the root or created from a parent branch in case of all other branches) and enters the cycle of metaepochs. Metaepoch is a set number of generations evolving in a classical way for genetic algorithms (as presented in Fig. 8). After metaepoch, if certain conditions are fulfilled, a new branch is created and evolves in the same way.

The implementation of HGS created by Kołodziej et al. [188,189] was based on binary encoding. To increase the performance of the search, Semczuk and Wierzba [190] created the HGS implementation with the floating-point encoding (HGS-FP). Together with the new encoding, the authors introduced new scaling of the algorithm, normal mutation and simple phenotypic cross-over, as well as several minor changes. The floating-point (real number) encoding is more efficient than the binary one, due to the conservation of the natural (topological) space where all variables are real numbers.

In their work [190], authors proved that using HGS-FP one can find the global optima more quickly and accurately for 10-dimensional and 20-dimensional functions than while using other genetic algorithms (SGA, ESGA, Genitor, I-SGA, I-ESGA, I-Genitor, binary HGS). The already implemented parallel version of HGS-FP [191] allows further decrease of the computation time.

HGS-FP has been used in the field of chemistry, namely for the optimization of Darken interdiffusion coefficients in *Si-Ge* nano-films [192]. HGS allows approximating the variable diffusivities in multicomponent systems with use of Generalized Darken Method [193]. The diffusion in the amorphous semiconductors (e.g. *Si-Ge* alloy) is currently of scientific importance, related to the potential applications in microelectronics [194,195].

In publications II and VI it is shown how to combine the HGS-FP and the NPP model. The resulting NPP-HGS method was used to solve the inverse problems i.e. to find the optimal parameters for achieving the best detection limit of an ISE and to find the parameters necessary to obtain given impedance spectrum.

The NPP-HGS method could be also used for solving other problems related to the analytical applications of ISE. In particular, the advantages of time-dependent selectivity can be exploited, disadvantages of poor response can be diagnosed and avoided or optimized design of ISEs can be undertaken.

3.7.1. NPP-HGS and Detection Limit

The cases described in chapter 3.3. are of the "normal problem" type ("What is the value of the detection limit if we have a certain set of NPP parameters?"). Equally, or maybe more important is the inverse problem, namely "Which set of NPP parameters produces the best detection limit?" Inverse problem, estimating these NPP parameters in order to obtain the lowest detection limit was presented in publication II.

As was shown in chapter 3.3., the concentration of the main ion in the inner solution of a plastic membrane ISE, as well as the measuring time, has very significant influence on the value of the detection limit. Finding the optimal values of these parameters may have a crucial impact on the design of ISEs.

In the NPP-HGS method used in publication II, we defined the fitness function as the value of the detection limit obtained using the NPP model for two variable parameters - the preferred ion concentration in the inner solution and the time of measurement (while all the other parameters are kept constant). HGS-FP optimized this function for the individuals represented by the values of these two parameters.

Fig. 4 in publication II shows a contour plot of the detection limit vs. the measurement time and the concentration of the preferred ion in the inner solution. The concentration is plotted on the x-axis, the measuring time on the y-axis. The detection limit is depicted with the help of different colour intensities (the darker the colour, the lower the detection limit). The local/global minima can be read from the plot. In order to obtain such contour plot, 1200 calibration curves had to be calculated and the total calculation time was 15 days.

The NPP-HGS method was able to find all the minima on the map significantly faster, i.e. it needed to calculate only 100 calibration curves in order to achieve this task. Individuals created during the solution of presented problem are visible as points in Fig. 6 in publication II.

The "brute force" approach for solving an inverse problem, presented for the first time in [89], requires a considerably large computational effort, which is exponentially proportional to the number of investigated parameters. In case more than two parameters are optimized the calculation time increases to few months or even years. Thus, we need a more advanced approach, i.e. the NPP-HGS method.

To further demonstrate the effectiveness of the NPP-HGS method the optimization of three parameters (concentration of the preferred ion in the inner solution, diffusion

coefficient of the preferred ion in the membrane and the time of measurement) was made. The results are presented in Fig. 7 in publication II. This result would be very unfeasible to obtain by the brute force approach. We would have to calculate 11 000 calibration curves which would take around four months.

The presented calculations show a great future potential for the NPP model combined with the HGS-FP used to facilitate the design of ISEs with a lower detection limit and in particular provide recommendations concerning analytical robustness when using ISEs for measurements in low concentrations.

3.7.2. NPP-HGS and Impedance Spectroscopy

The use of evolutionary algorithms has already been indicated as a potential tool for the interpretation of electrochemical impedance spectra. Yang et. al [196] used Simple Genetic Algorithm (SGA) to estimate the initial parameters of the elements of equivalent circuits for further calculations with the use of non-linear regression procedure. Kanoun et al. [197] presented a comparison between evolutionary strategy and Levenberg-Marquardt method for finding the parameters of the elements of equivalent circuits. Comparing the circuits with different complexity levels, they found that evolutionary strategy gives better results for simpler circuits. For more complex ones, using the results of evolutionary strategy combined with Levenberg-Marquardt method reached better and more reliable results, compared to both methods alone (hybrid solution profited from different sensitivities of both methods).

The NPP-HGS method allows the interpretation of impedance spectra of ISE, relating the shape of impedance spectrum and the impedance values to the physicochemical parameters of the system, such as diffusion coefficients, concentration of species of all components, membrane thickness and heterogeneous rate constants.

In this method, HGS-FP is used to optimize the calculated reference spectra by the inverse method. We define the fitness function as a difference between the analysed spectrum and the spectrum calculated using the NPP model for the set of optimized parameters represented by given individual differs from the reference one:

$$fitness = \sum_j g^j \left| \mathrm{Re}\left(Z^j_{calc}\right) - \mathrm{Re}\left(Z^j_{ref}\right) \right| + \sum_j h^j \left| \mathrm{Im}\left(Z^j_{calc}\right) - \mathrm{Im}\left(Z^j_{ref}\right) \right| \qquad (54)$$

where: g^j and h^j are the weight functions, Z^j_{calc} and Z^j_{ref} are the calculated and reference complex impedance values at *j-th* frequency.

Such formulated NPP-HGS method was presented in publication VI and applied to find the parameters in multi-component ionic solutions, i.e. to approximate the diffusion coefficients for complex electrochemical systems.

The reference spectra were created using the NPP model, where the system was perturbed by a sinusoidal excitation signal (see chapter 3.6.). These spectra, with the added noise of different level (0%, 7%, 15% and 30%), were used to test the NPP-HGS algorithm. The aim was to obtain the original physicochemical parameters used to generate the reference spectra.

The results, obtained for reference spectra with 0% noise, clearly demonstrate that HGS-FP algorithm (and consequently NPP-HGS method) is a stochastic one, i.e. parameters calculated during two successive runs have different values, but still remain close to the reference ones. The NPP-HGS method found the expected values of the optimized parameters also when the level of noise was high. This proves that the NPP-HGS method can be used to obtain meaningful values of the physical parameters of electrochemical sensors.

It was shown that impedance spectra analysed using the NPP-HGS method could be a source for physicochemical characteristic of ISEs, giving a possibility to assess the properties of ISEs and their response mechanism. The NPP-HGS method allows calculation of the most accurate solution of the inverse problem and can be effectively used to facilitate the process of finding the parameters for the optimal ISE performance.

Although, in publication VI, we limited the optimization to diffusion coefficients, the presented method allows us to find parameters such as membrane thickness, dielectric permittivity, concentrations (in the internal reference solution and in the sample) of all components, as well as the heterogeneous rate constants. NPP-HGS combined with EIS can be used as a novel method of estimating the heterogeneous rate constants, alternatively to the use of voltammetric methods for estimation of those constants [198,199,200,201].

3.8. Other Interesting Applications of NPP Model

In this chapter some other possible applications of the NPP model are presented. The overshoot time-dependent response of ISE as well as the effect of the anionic sites is investigated. One of the most interesting applications of NPP, the description of biological systems is also indicated.

Another possible application of NPP, not mentioned in the following subchapters, is in chrono-potentiometric measurements. This method differs from classical potentiometry by the applied external current. As the systems with applied current were already studied (Impedance Spectroscopy in chapter 3.6.), the possible description of electrodes applied in chrono-potentiometry is relatively easy and might be a subject of the future work.

3.8.1. Overshoot Response of ISE

Extensive studies on the dynamic behaviour of potentiometric ion sensors were initiated mostly by groups working on the development of continuous monitoring systems [202,203,204,205] and accompanied with the elaboration of appropriate theories [205,206,207]. In the theories by Markovic and Osburn [205] and by Morf et. al [208] it was recognized that diffusion processes are crucial for the response time of many electrode systems.

The effect called overshoot potentiometric response, first observed by Lindner *et al.* [209] in 1982, is a characteristic transient-state potential response for the solid state ISEs. It is the effect of the presence of the diffusion layer, as is already shown in works of Lindner [210], Lewenstam [211, 212] and Bakker [213]. This time-dependent response has been observed for ISE with magnesium-selective PCV-membranes [214] and conducting polymers films doped with adenosine triphosphate [215], heparin [216] or amino-acids [217].

In [217], authors investigated ISE with the CP doped with asparagine and glutamine which is sensitive to calcium and magnesium ions. The basic sample solution contained a mixture of magnesium and calcium chloride salts, with constant Mg^{2+} concentration when the response to calcium was tested, and constant Ca^{2+} concentration when the response to magnesium was tested. The time-dependent potential profiles have totally different shapes. They are either monotonic (in case of Mg^{2+} changes) or show overshoot (in case of Ca^{2+} changes). The reason for that is the difference in mobility of this two ions and the difference in hydratation energy of these two ions [215,216], causing the local excess of Mg^{2+} near the surface of ISE after the calcium concentration change in the sample or the local deficiency of Ca^{2+} near the surface of ISE after the magnesium concentration change.

The time-dependent overshoot potential response of potentiometric sensors was studied using DLM [217] and the behaviour of ISE described above was correctly predicted by the model.

In publication III, the experimental results of Gratzl and Lindner [210] were compared with the ones obtained using multi-layer NPP model (chapter 3.1.). The potential responses as functions of time for the theoretical and the experimental ISE show qualitative agreement. The quantitative agreement can be achieved provided that we know real physical and chemical parameters (i.e., diffusion coefficients, rate constants, etc.). This may be obtained by solving the suitable inverse problem, as it is described in chapter 3.7.

3.8.2. Influence of Ionic Sites

Recently Silvester et al. [218] presented a potentiometric method to monitor ion-exchange properties (or "purity") of an organic solvent containing a lipophilic electrolyte. Such solvent was treated as a liquid membrane between two aqueous solutions with different electrolyte activities. The system analyzed in their work corresponds to ISE with a membrane containing two ion-exchangers with the opposite charges: the cation-exchanger R^- (representing tetrakis(4-chlorophenyl)borate ion $TClPB^-$) and anion-exchanger R^+ (representing tetradodecyloamonium ion $TDDA^+$).

These authors observed that in the presence of R^- in the membrane, the generated potential is positive (cation-sensitive ISE). When R^+ is added at a concentration in excess of R^-, the membrane potential switches from cationic to anionic response. These theoretical discussions were confirmed with the experiment, by titration of $TDDA^+$ into a solution containing the constant concentration of $TClPB^-$.

The results, presented in the Fig. 9a, show that the change from cationic to anionic response for experimental ISE is more gradual comparing with the rapid jump change expected from the theory based on PBM. In order to investigate this change of response, we used the NPP model (with one layer) for the description of above system. Results shown in Fig. 9b clearly shows that NPP can not only correctly describe a gradual change of potential near the point $c^M_{R^-} = c^M_{R^+}$, but also can relate the range of concentrations in which this gradual change takes place to the heterogeneous rate constants at the membrane boundaries.

In the calculations, the heterogeneous rate constants for both ions entering the membrane were set to $\overrightarrow{k^0_{K^+}} = \overrightarrow{k^0_{Cl^-}} = \overleftarrow{k^1_{K^+}} = \overleftarrow{k^1_{Cl^-}} = 10^{-3} m \cdot s^{-1}$. The heterogeneous rate constants for these two ions leaving the membrane were changed between $\overleftarrow{k^0_{K^+}} = \overleftarrow{k^0_{Cl^-}} = \overrightarrow{k^1_{K^+}} = \overrightarrow{k^1_{Cl^-}} = 10^{-8} m \cdot s^{-1}$ and $\overleftarrow{k^0_{K^+}} = \overleftarrow{k^0_{Cl^-}} = \overrightarrow{k^1_{K^+}} = \overrightarrow{k^1_{Cl^-}} = 10^{-6} m \cdot s^{-1}$. As shown in Fig. 9b, when the ions are allowed to leave the membrane faster, the range of the gradual change becomes significantly bigger.

Lipophilic ions can disturb the response of ISE signal by direct-exchange and site-competing mechanism. These effects can be either treated as interferences [219,220] or can be advantageously utilized, e.g. to obtain ISE sensitive to lipophilic ions [221], prevention of Donnan exclusion failure [222].

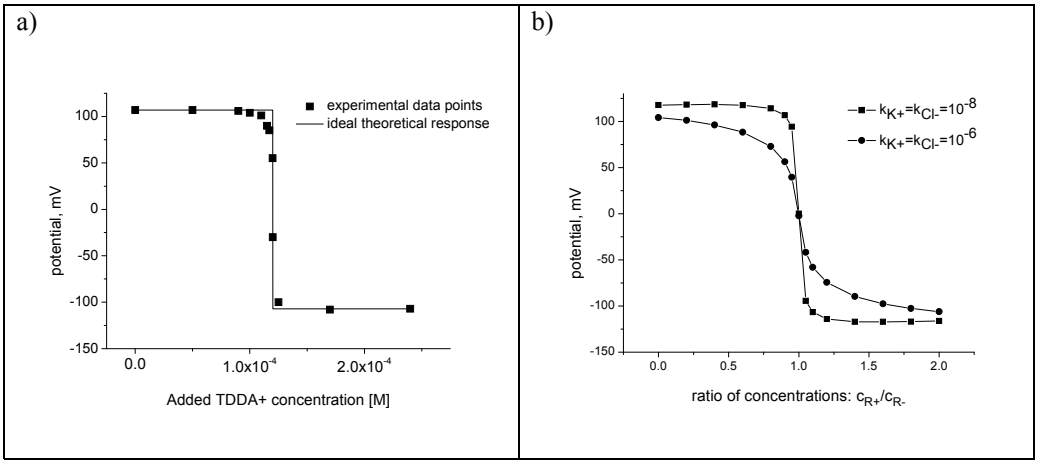

Figure 9. *Potential Response depending on the amount of anion-exchanger with the constant concentration of cation-exchanger in the membrane. a) results obtained from experiment and using PBM, b) results obtained using the NPP for different values of heterogeneous rate constants.*

In the work of Lewenstam et al. [223], the authors presented the slope of K^+-sensitive ISE after different intervals in contact with the Aliquat 336 (quaternary ammonium chloride) emulsion. A very characteristic feature of their results is the gradual decrease of the slope, which initially shows the cation-sensitive response and finally become anion-sensitive. This corresponds to the conversion of the membrane by quaternary ammonium ions. This effect is analogical to the one obtained by the titration of $TDDA^+$ [218] and can be described using the NPP model.

Application of NPP in cases described above as well as other more general cases, where the properties of lipophilic interferents have the crucial influence on the potentiometric response, will be a subject of future research.

3.8.3. Biological Systems

Mueller et al. [224] introduced the bilayer lipid membranes as primitive models of biological membranes. The thickness of such membranes is on the order of only 10nm. The theoretical description of lipid bilayers was developed mainly by the group of Eisenman [225]. The classical approach by Läuger and Stark [226], where the membrane interior was considered as a single sharp energy barrier, was not capable of rationalizing quantitatively the carrier-induced ion transport behaviour of lipid bilayers. The extended theory, by Hladky [227,228] and Ciani [229,230], allows for a voltage dependence of the interfacial reactions as well as for the trapezoidal shape of energy barrier for translocation of the complexes. The theories used for the description of lipid bilayer are described in more detail in [2].

Computations using the NPP model, widespread in chemistry and material science, can be also useful tool in the description of biological system. The NPP model has the potential to reopen frontiers in the study of variety of the problems related to the electrochemistry of biological membranes [88].

It can serve for the description of lipid bilayers assuming them as a continuous environment. Morf et al. [231] presented a numerical method for the description of the extremely thin membranes. They used the full form of NPP, i.e. without the substitution of Poisson equation with total current equation in the form given by Cohen and Cooley [65]:

$$\begin{cases} \dfrac{\partial c_i}{\partial t}(x,t) = -\dfrac{\partial J_i}{\partial x}(x,t) \\ \dfrac{\partial^2 \varphi}{\partial x^2}(x,t) = -\dfrac{F}{\varepsilon_0 \varepsilon} \sum_i z_i c_i(x,t) \\ \quad \text{where:} \\ J_i(x,t) = D_i \dfrac{\partial c_i}{\partial x}(x,t) + \dfrac{F}{RT} D_i z_i c_i \dfrac{\partial^2 \varphi}{\partial x^2}(x,t) \end{cases} \tag{55}$$

Following this approach to NPP modelling, the NPP model for the description of the theoretical biological membrane, e.g. cellular wall, was developed. We have considered a system that consists of three layers: the exterior of the cell, the lipid membrane and the interior of the cell.

It is assumed that all changes in electrical potential take place inside the membrane (diffusion potential of the layers is negligible). In the diffusion layers outside and inside the cell pure Fickian diffusion is assumed, so the concentrations are calculated using the mass

balance equation and Fick's expression for flux (eq. 15, see chapter 2.3.). For the description of the concentration and potential changes inside the membrane we use mass balance equation and Poisson equation, respectively and the flux is given by the Nernst-Planck equation. For the membrane phase the set of PDEs given with eq. 56 is obtained.

On the left and right boundary of the system we assume constant value of the concentrations of each component $c_i^0 = const$ and $c_i^4 = const$ (Dirichlet boundary conditions). The values of fluxes at the boundaries of the membrane are calculated using Chang-Jaffe boundary conditions [101] (in the form given by eq. 28, see chapter 3.1.). At the boundaries of the membrane constant potential values φ_L and φ_R are assumed.

Certain ion I^+ is transported from exterior of the cell into its interior and this process may be of vital importance for the organism. As known from biological experiments, the electrical potential can be formed on the membrane due to powerful processes independent of I^+ transport [232]. We assume constant potential values φ_L and φ_R at the boundaries of the membrane.

Finally, in the interior of the cell the reaction occurs, which is reflected by adding the reaction term to mass balance equation (see eq. 53 in chapter 3.4.). Set of PDE was transformed to a set of ODE using Method of Lines. This set of ODE was then integrated using the Euler's method. Effective algorithm was implemented in C++ language.

A set of the calculations was performed in order to simulate the behaviour of the presented theoretical biological system. Influence of different parameters was discussed. Time necessary to reach steady state was investigated. For presented set of system time $t_{END} = 10s$ was sufficient to obtain equilibrium.

The values of the external solution concentration of I^+ and the membrane potential determine the value of the flux. The higher the concentration or the more negative the potential, the bigger the tendency of the ions to enter the cell. This effect can is depicted in Fig. 10 using the concentration profiles obtained for different values of membrane potential

Also the influence of the ratio of the reaction rate constants ($k_{I,as}$ and $k_{I,dis}$) and the value of initial IX concentration on the right side of the system were discussed. The lower the ratio of the reaction rate constants, the lower the value of the concentration of I^+ at the right boundary of the system and therefore the lower the tendency of this ion to enter the cell.

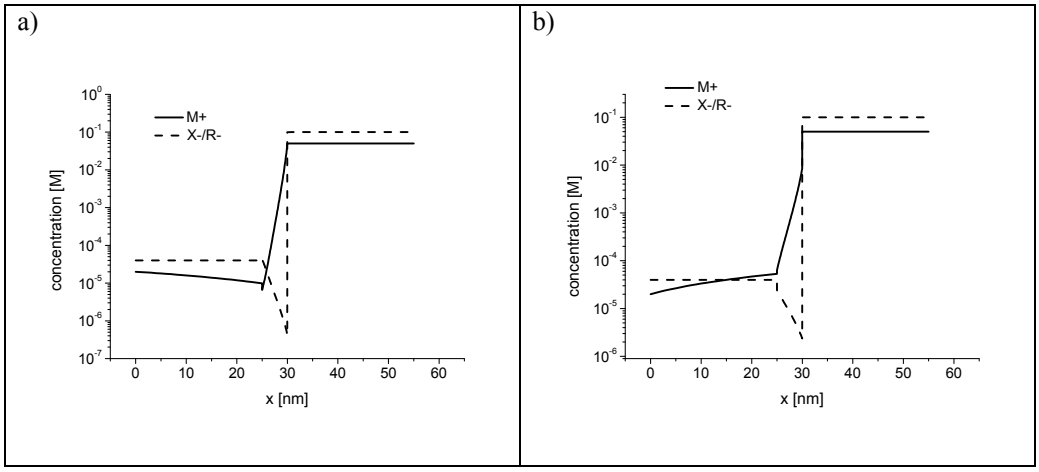

Figure 10. *Concentration profiles in the system describing cellular wall obtained using the NPP model for different values of membrane potential a) -120mV, b) -60mV. System consisting of 5µm lipid bilayer surrounded by two 25µm diffusion layers.*

The model created, can be used for the description of real biological systems in the future. The case of particular interest and the subject of future work is the transport of calcium to mitochondrion. The concentration of free calcium in the cell can regulate an array of reactions and is important for signal transduction in the cell. Mitochondria can transiently store calcium, a contributing process for the cell's homeostasis of calcium [233].

4. Conclusions

Various mathematical models used for the description of potentiometric ion sensors were presented and compared. The physical relevance of the NPP model for multi-layer and multi-component systems is much higher than that of the total equilibrium or local equilibrium models. Owing to all the assumptions of a mathematical, numerical and physicochemical nature, the NPP model (as every model in analytical chemistry [234]) is approximate. Nevertheless, at this level of approximation it is possible to analyze a variety of electrochemical systems.

It may seem that the NPP model is formally complicated, while the other models (described in chapter 2.) are relatively simple. As a matter of fact, the situation is quite the opposite [44]. Once the NPP is implemented, it serves as a flexible and powerful tool that enables inspection of numerous cases such as those described in this thesis, i.e. liquid-junction potential in reference electrodes, potentiometric response of ion-selective electrodes with ion-exchanger and neutral-carrier membranes, electrochemical impedance spectroscopy and other applications. With more idealized models, different cases must be considered separately and in each case several (sometimes dubious) assumptions must be made.

The trends found using the simpler models are confirmed by the NPP and are of general validity for the formation of liquid-junction potential and the description of ISEs behaviour. Simplified models (in the cases, where they apply) agree satisfactorily with the general NPP model, although they do not apply to the complex practical cases, such as polyvalent ions or large number of ions.

The NPP model allows the description of many types of ISE. The NPP modelling of ion-exchanger ISEs has been widely described in the literature. Inclusion of the reaction term in the model allows more adequate description of the neutral-carrier electrodes. NPP allows the description of various interesting phenomena, such as overshoot response of ISE or the effect of oppositely charged ion-exchangers. The possible future applications for the description of the biological membranes are also indicated.

The NPP model is also applicable to describe Electrochemical Impedance Spectra. Two different methods (direct current perturbation and sinusoidal excitation) were used in order to generate theoretical spectra and compared.

For the description of some more complex electrochemical systems, e.g. Pb^{2+}-sensitive solid-contact ISE, NPP is the only applicable model and qualitatively agrees

with the experiment. To obtain quantitative agreement, an inverse problem has to be formulated.

The formulation of the inverse problem, by combining the Hierarchical Genetic Strategy with real number encoding (HGS-FP) and the NPP model, allows the optimal parameters of ISE to be found and it was successfully applied for investigating the best detection limit of ISE or the best agreement between the theoretical and experimental EIS plots. The computational effort is much smaller for the NPP-HGS method than for the brute force approach. Results obtained with the NPP-HGS method to find the parameters of the system based on EIS plot, shows that the presented method can find an optimal fit even in the presence of noise.

The results, presented in this thesis, show the great potential of possible applications of the NPP model as well as the NPP-HGS method for the description of ion sensors and other electrochemical systems.

5. References

[1] E. Bakker, M.Telting-Diaz; *Anal. Chem.* **2002**, 74, 2781.
[2] W.E. Morf; *The Principles of Ion-Selective Electrodes and of Membrane Transport*; Akadémiai Kiadó: Budapest, 1981.
[3] J. Bobacka, A. Ivaska, A. Lewenstam; *Chemical Reviews* **2008**, *108*, 329.
[4] G. Trümpler; *Z. Phys. Chem.* **1921**, 99, 9.
[5] I.M. Kolthoff, H.L. Sanders; *J. Am. Chem. Soc.* **1937**, 59, 416.
[6] E. Pungor, E. Hollós-Rokosinyi; *Acta Chim. Hung.* **1961**, 27, 63.
[7] M.S. Frant, J.W. Ross Jr.; *Science* **1966**, 154, 1553.
[8] E. Pungor, K. Tóth; *Pure Appl. Chem.* **1973**, 34, 105.
[9] E. Pungor, K. Tóth; *Pure Appl. Chem.* **1973**, 36, 441.
[10] E. Pungor, K. Tóth; *Ion-Selective Electrodes in Analytical Chemistry* (H. Freiser ed.), Plenum Press, New York, 1978.
[11] A. Shatkay; *Anal. Chem.* **1967**, 39, 1056.
[12] R. Bloch, A. Shatkay, H.A. Saroff; *Biophys. J.* **1967**, 7, 865.
[13] G.J. Moody, J.D.R. Thomas; *Selective Ion Sensitive Electrodes,* Merrow, Watford (GB) 1971.
[14] E. Bakker, P. Bühlmann, E. Pretsch; *Chem. Rev.* **1997**, 97, 3083.
[15] P. Bühlmann, E. Pretsch, E. Bakker; *Chem. Rev.* **1998**, 98, 1593.
[16] R.D. Purves; *Microelectrode Methods for Intracellular Recording and Ionophoresis;* Academic Press: London, 1981.
[17] D. Ammann; *Ion-selective microelectrodes: Principles, Design and Applications;* Springer-Verlag: Berlin, 1986.
[18] A. Takahashi, P.Camacho, J. Lechleiter, B. Herman; *Physiol. Rev.* **1999**, 79, 1086.
[19] J. Huller, M.T. Pham, S. Howitz; *Sens. Actuators, B* **2003**, 91, 17.
[20] J.E. Zachara, R. Toczyłowska, R. Pokrop, M. Zagórska, A. Dybko, W. Wróblewski; *Sens. Actuators, B* **2004,** 101, 207.
[21] S.S.M. Hassan. H.E.M. Sayour, S.S. Al.-Meherezi; *Anal. Chim. Acta* **2007**,581,13.
[22] A.J. Miller, S.J. Cookson, S.J. Smith, D.M.J. Wells; *J. Exp. Botany* **2001,** 52, 541.
[23] P.W. Dierkes, S. Neumann, A. Muller, D. Gunzel, W.-R. Schlue; *New Trends Electrochem. Technol.* **2003,** 2, 526.
[24] P.W. Dierkes, S. Neumann, G. Klees, W.-R. Schlue; *Electrochim. Acta* **2003**, 48, 3373.
[25] W.A. Timms, M.J. Hendry; *Ground Water Monit. Rem.* **2004**, 24, 67.
[26] J.J. Wang P.L. Bishop; *Envinron. Technol.* **2005**, 26, 381.
[27] M.J. Dole; *Am. Chem. Soc.* **1931**, 53, 4260.
[28] B.P. Nikolsky; *Acta Phys.-Chim. USSR* **1937**, 7, 597.
[29] O.K. Stefanova, M. M. Shultz, E. A. Materova, B.P. Nikolsky; *Viest. Leningr. Univ.* **1963**, 4, 93.
[30] M.M. Shultz, O.K. Stefanova; *Viest. Leningr. Univ.* **1967**, 6, 103.
[31] F. Conti, G. Eisenman; *Biophys. J.*, **1965**, 5, 247.
[32] F. Conti, G. Eisenman; *Biophys. J.*, **1965**, 5, 511.
[33] IUPAC; *Pure Appl. Chem.* **1976**, 48, 129.
[34] IUPAC; *Pure Appl. Chem.* **1994**, 66, 2527.
[35] T. Sokalski, A. Lewenstam; *Electrochem. Comm.* **2001**, 3, 107.
[36] F. G. Donnan; *Z. Elektrochem.* **1911**, 17, 572.
[37] F. G. Donnan; *Chem. Rev.***1924**, 1, 73.
[38] E.A. Guggenheim; *J. Phys. Chem.* **1929**, 33, 842.
[39] B.P. Nikolsky; *J. Phys. Chem.* (USSR) **1937**, 10, 495.
[40] G. Eisenman; *Nat. Bur. Of Standards Spec.,* Publ. 314; in R.A. Durst; *Ion-Selective Electrodes,* Washington D.C., 1969.
[41] T. Kakiuchi; *Anal. Chem.* **1996**, 68, 3654.
[42] W.E. Morf, M. Badertscher, T. Zwickl, N.F. de Rooij, E. Pretsch; *J. Phys. Chem. B* **1999**, 103, 11346.

[43] K.N. Mikhelson, A. Lewenstam; *Anal. Chem.* **2000**, 72, 4965.
[44] T. Sokalski, P. Lingenfelter, A. Lewenstam; *J. Phys. Chem. B* **2003**, 107, 2443.
[45] A. Lewenstam; *Scand. J. Lab. Clin. Invest.* **1994**, 54, 11.
[46] E. Pungor; *Talanta* **1997**, 34, 1505.
[47] A. Lewenstam; *PhD Thesis*, Warsaw University, Poland, 1977.
[48] A. Hulanicki, A. Lewenstam; *Talanta* **1977**, 24, 171.
[49] A. Hulanicki, A. Lewenstam; *Anal. Chem.* **1981**, 53, 1401.
[50] A. Hulanicki, A. Lewenstam; *Talanta* **1982**, 29, 661.
[51] W.E. Morf; *Anal. Chem.* **1983**, 55, 1165.
[52] A. Lewenstam, A. Hulanicki, T. Sokalski; *Anal. Chem* **1987**, 59, 1539.
[53] L. Icheva, K. Cammann; *Fresenius J. Anal. Chem.* **1985**, 320, 664.
[54] B. Paczosa-Bator, T. Blaz, J. Migdalski, A. Lewenstam; *Bioelectrochem.* **2007**, 71, 66.
[55] B. Fu, E. Bakker, J.H. Yun, V.C. Yang, M. Meyerhoff; *Anal. Chem.* **1994**, 66, 2250.
[56] J. Langmaier, E. Samcova, Z. Samec; *Anal. Chem.* **2007**, 79, 2892.
[57] T. Sokalski, T. Zwickl, E. Bakker, E. Pretsch; *Anal. Chem.* **1999**, 71, 1204.
[58] T. Sokalski, A. Cereza, T. Zwickl, E. Pretsch; *J. Am. Chem. Soc.* **1997**, 119, 11347.
[59] W.E. Morf, E. Pretsch, and N.F. de Rooij; *J. Electroanal. Chem.* **2007**, 602, 43.
[60] Crank and J; *Mathematics of Diffusion*, Oxford University Press, 1970.
[61] M.E. Glicksman; *Diffusion in Solids: Field Theory, Solid-State Principles and Applications*, John Wiley and Sons, 2000
[62] J.S. Kirkaldy, D.J. Young; *Diffusion in the Condensed State*, The Institute of Metals, London, 1985.
[63] A. Radu, A.J. Meir, E. Bakker; *Anal. Chem.* **2004**, 76, 6402.
[64] J.W. Perram, P.J. Stiles; *Phys. Chem. Chem. Phys.* **2006**, 8, 4200.
[65] H. Cohen, J. Cooley; *Biophys. J.* **1965**, 5, 145.
[66] E. Samson, J. Marchand, J.-L. Robert, J.-P. Bournazel; *Int. J. Numer. Meth. Engng.* **1999**, 46, 2043.
[67] M. Planck; *Ann. Phys. Chem.,***1980**, 40, 561.
[68] R. Schlögl; *Z. Phys. Chem.* **1954**, 1, 305.
[69] F. Helfferich; *Ion Exchange*; McGraw-Hill: USA, 1962.
[70] T. Teorell; *Progress in Biophysics. and Biophys. Chem.* **1953**, 3, 305.
[71] D.E. Goldman; *J. Gen. Physiol.* **1943***,* 27, 37.
[72] A.D. MacGillivray; *J. Chem. Phys.* **1968**, 48, 2903.
[73] A.D. MacGillivray, D. Hare; *J. Theor. Biol.* **1969**, 25, 113.
[74] J.R. Sandifer, R.P. Buck; *J. Electroanal. Chem.* **1974**, 56, 385.
[75] J.P. McKelvey; *Solid State and Semiconductor Physics,* Krieger: Malabar, FL, 1982.
[76] J. Marchand, B. Gérard, A. Delagrave; *Ion transport mechanism in cement-based materials*. In: *Materials Science of Concrete,* vol.V, J.P. Skalny (ed.), *Am. Ceram. Soc.,* Ohio 1998, (p. 307).
[77] N. Lakshminarayanaiah; *Equations of Membrane Biophysics;* Academic: New York. 1984.
[78] R.F. Probstein; *Physicochemical Hydrodynamics*, Butterworth: Stoneham, NA, 1989.
[79] D.L. Scharfetter, D.L. Gummel; *IEEE Trans. Elect. Dev. ED-16* **1969**, 64.
[80] J.W. Thomas; *Numerical Partial Differential Equations: Finite Difference Methods*, Springer Verlag, New York, 1995, p. 84.
[81] T.R. Brumleve, R.P. Buck; *J. Electroanal. Chem.* **1978**, 90, 1.
[82] A. Quarteroni, R. Sacco, F. Saleri; *Numerical Mathematics*, Springer Verlag, New York, 2000, p. 281.
[83] S. Mafé, J. Pellicer, V.M. Aguilella; *J. Phys. Chem.* **1986**, 90, 6045.
[84] S. Mafé, J. Pellicer, V.M. Aguilella; *An. Fis., Ser. B* **1987**, 83, 96.
[85] J.A. Manzanares, S. Mafé, J. Pellicer; *J. Phys. Chem.* **1991**, 95, 5620
[86] A.K. Kontturi, K. Kontturi, S. Mafé, J.A. Manzanares, P. Niinikoski, M. Vouristo; *Langmuir* **1994**, 10, 949.
[87] K. Kontturi, S. Mafé, J.A. Manzanares, J. Pellicer; *J. Electroanal. Chem.* **1994**, 378, 111.
[88] P. Lingenfelter, I. Bedlechowicz-Śliwakowska, T. Sokalski, M. Maj-Żurawska, A. Lewenstam; *Anal. Chem.* **2006**, 78, 6783.

[89] T. Sokalski, W. Kucza, M. Danielewski, A. Lewenstam; *Anal. Chem.* **2009**, 81, 5016.
[90] W.D. Murphy, J.A. Manzanares, S. Mafé, H.Reiss; *J. Phys. Chem.* **1992**, 96, 9983.
[91] J.O'M. Bockris, A.K.N. Reddy; *Modern Electrochemistry;* Plenum: New York, 1970.
[92] W.E. Schiesser; *The Numerical Method of Lines: Integration of Partial Differential Equations*, Academic Press, San Diego, 1991.
[93] C.W. Cear; *Numerical Initial Value Problems in Ordinary Differantial Equations;* Prentice-Hall: Old Tappan, NJ, 1971.
[94] A.C. Hindmarsh; *ACM SIGNUM Newslett.* **1980**, 15, 10.
[95] S. Mafé, J.A. Manzanares, P. Ramirez; *Phys. Rev. A* **1990**, 42, 6245.
[96] R. Filipek; *Polish Ceram. Bull.* **2005**, 90, 103.
[97] P. Lingenfelter, T. Sokalski, A. Lewenstam; *Unbiased selectivity coefficients: new insights from the Nernst–Planck–Poisson model*, in: *International Conference on Electrochemical Sensors MATRAFURED 2005*, Mátrafüred, Hungary,13.11.2005.
[98] J.J. Jasielec; *Master Thesis*, AGH-UST/ÅAU, Kraków/Åbo 2008.
[99] W. Kucza, M. Danielewski, A. Lewenstam; *Electrochem. Comm.* **2006**, 8, 416.
[100] B. Grysakowski, B. Bozek, M. Danielewski; *Diffus. Defect Data [Diffusion in Solids and Liquids III]* **2008**, 113, Pt. A 273.
[101] H. Chang, E. Jaffe; *J. Chem. Phys.* **1952**, 20, 1071.
[102] J.L. Harden, J.L. Viovy; *J. Contr. Released* **1996**, 38, 129.
[103] M. Sodel; *Master Thesis*, AGH-UST, Kraków 2007.
[104] W.E. Schiesser; *The Numerical Method of Lines*, Academic Press, San Diego, 1991.
[105] V.M. Volgin, A.D. Davydov; *J. Electroanal. Chem.* **2007***,* 600, 171.
[106] E. Hairer, G. Wanner; *J. Comput. Appl. Math.* **1999**, 111, 93.
[107] L.K. Bieniasz; *J. Electroanal. Chem.* **1999**, 469, 97.
[108] W.H. Nernst; *Z. Phys. Chem.* **1889**, 4, 165.
[109] M. Planck; *Ann. Phys. Chem.* **1980**, 39, 161.
[110] E.J.F. Dickinson, L. Freitag, R.G. Compton; *J. Phys. Chem. B* **2010**, 114, 187.
[111] D.A. MacInnes; *The Principles of Electrochemistry,* Dover: New York, 1961.
[112] E.A. Guggenheim; *J. Am. Chem. Soc.* **1930**, 52, 1315.
[113] J.L. Jackson; *J. Phys. Chem.* **1974**, 78 (20), 2060.
[114] R.N. Goldberg, H.S. Frank; *J. Phys. Chem.* **1972**, 76, 1758.
[115] J. Horno, J. Castilla, C.F. Gonzalez-Fernandez; *J. Phys. Chem.* **1992**, 96, 854.
[116] D.R. Hafemann; *J.Phys. Chem.* **1965**, 69, 4226.
[117] A. Lewenstam; *Scand. J. Clin. Lab. Invest., Suppl.* **1994**, 54, 11.
[118] W.E. Morf; *Anal. Chem. 1977, 49 (6), 810.*
[119] P. Henderson; *Z. Phys. Chem.* **1907**, 59, 118.
[120] P. Henderson; *Z. Phys. Chem.* **1908**, 63, 325.
[121] J. J. Lingane; *Electroanalytical Chemistry*, 2nd edition; Wiley: New York, 1998.
[122] H.J. Hickman; *Chem. Eng. Sci.* **1970**, 25, 381.
[123] K.R. Ward, E.J.F. Dickinson, R.G. Compton; *J. Phys. Chem. B* **2010**, 114, 4521.
[124] A. Lewenstam; *Anal. Proc.* (London) **1991**, 28, 106.
[125] A. Lewenstam, M. Maj-Żurawska, A. Hulanicki; *Electroanalysis* **1991**, 3, 727.
[126] K. Zhurov, E.J.F. Dickinson, R.G. Compton; *J. Phys. Chem. B* **2011**, 115, 6909.
[127] K. Zhurov, E.J.F. Dickinson, R.G. Compton; *J. Phys. Chem. B* **2011**, 115, 12429.
[128] R.P. Buck, E. Lindner; *Pure Appl. Chem.* **1994**, 66, 2527-2536.
[129] W.E. Morf, G. Kahr, W. Simon; *Anal. Chem.* **1974**, 46, 1538-1543.
[130] A. Hulanicki, A. Lewenstam; *Talanta* **1976**, 23, 661-663.
[131] A. Lewenstam; *J. Solid State Electrochem.*, **2011**, 15, 15.
[132] T. Sokalski, M. Maj-Żurawska, A. Hulanicki, A. Lewenstam; *Electroanalysis* **1999**, 11, 632.
[133] T. Sokalski, A. Ceresa, M. Fibioli, T. Zwickl, E. Bakker, E. Pretsch; *Anal. Chem.* **1999**, 71, 1210.
[134] K.N. Mikhelson, A. Lewenstam; *Sens Actuators B* **1998***,* 48, 344.
[135] K.N. Mikhelson, A. Lewenstam, S.E. Didina; *Electroanalysis* **1999***,* 11, 793.

[136] W.E. Morf, M. Badertscher, T. Zwickl, P.d.R.N.F. Reichmuth, E. Pretsch; *J. Phys. Chem. B* **2000**, 104, 8201.
[137] L. Michaelis, A. Fujita; *Biochem. Z.* **1925,** 158, 28.
[138] K. Sollner; *Z. Electrochem.* **1930**, 36, 36.
[139] R. Beutner; *Physical Chemistry of Living Tissue and Life Processes*, Williams and Wilkins, Baltimore, 1933.
[140] T. Teorell; *Trans. Faraday Soc.* **1937**, 33, 1053.
[141] K.H. Meyer, J.F. Sievers; *Helv. Chim. Acta* **1936**, 19, 649 and 665.
[142] M. Maj-Żurawska, T. Sokalski, A. Hulanicki; *Talanta* **1988**, 35, 281.
[143] C. Moore, B.C. Pressman; *Biochem. Biophys.Res. Commun.* **1964**, 15, 562.
[144] Z. Štefanac, W. Simon; *Microchem. J.* **1967**, 12, 125.
[145] R.A. Durst; *Ion-Selective Electrodes,* Washington D.C., 1969.
[146] A. Lewenstam; *Clinical analysis of blood gases and electrolytes by ion-sensitive sensors*, in: *Electrochemical Sensor Analysis* (*Comprehensive Analytical Chemistry* vol. 49); S. Alegret. A. Merkoci (Eds.), Elsevier, Amsterdam, the Netherlands; Oxford, UK; Chapter 1, p. 5.
[147] M. Ngele, E. Bakker, E. Pretsch; *Anal. Chem.* **1999**, 71(5), 1041.
[148] E. Lindner, E. Graf, Z. Niegreisz, K. Tóth, E. Pungor, R.P. Buck; *Anal. Chem.* **1988**, 60, 295.
[149] R.W. Cattrall, H. Freiser; *Anal.Chem.* **1971**, 43, 1905.
[150] B.P. Nikolsky, E.A. Materova; *Ion-Sel. Electrode Rev.* **1985**, 7, 3.
[151] W. Wróblewski, A. Dybko, E. Malinowska, Z. Brzózka; *Talanta* **2004**, 63, 33.
[152] S.R. Lukow, S.P. Kounaves; *Electroanalysis* **2005**, 17, 1441.
[153] M. Fibbioli, K. Bandyopadhyay. S.-G. Liu, L. Echegoyen, O. Enger, F. Diederich, D. Gingery, P. Bühlmann, H. Persson, U.W. Suter, E. Pretsch; *Chem. Mater.* **202**, 14, 1721.
[154] E. Grygołowicz-Pawlak, K. Wyglądacz, S. Sęk, R. Bilewicz, Z. Brzózka, E. Malinowska; *Sens. Actuators, B* **2005**, 111-112, 310.
[155] J. Gallardo, S. Alegret, R. Muñoz, M. De-Román, L. Leija, P.R. Hernández, M. del Valle; *Anal. Bioanal. Chem.* **2003**, 377, 248.
[156] P.G. Veltsistas, M.I. Prodromidis, C.E. Efstathiou; *Anal. Chim. Acta* **2004**, 502, 15.
[157] M. Fouskaki, N.A. Chaniotakis; *Anal. Chem.* **2005,** 77, 1780.
[158] A. Cadogan, Z. Gao, A. Lewenstam, A. Ivaska, D. Diamond; *Anal. Chem.* **1992**, 64, 2496.
[159] T. Blaz, J. Migdalski and A. Lewenstam; *Talanta* **2000**, 52, 319.
[160] A. Michalska, A. Hulanicki, A. Lewenstam; *Analyst* **1994**, 119, 2417.
[161] A. Michalska, K. Maksymiuk; *Anal. Chim. Acta* **2004**, 523, 97.
[162] S. Anastasova-Ivanova, U. Mattinen, A. Radu, J. Bobacka, A. Lewenstam, J. Migdalski, M. Danielewski, D. Diamond; *Sens. Actuators B* **2010**, 146, 199.
[163] S. Yu, F. Li, W. Qin; *Sens. Actuators B* **2011**, 155, 919.
[164] J. Bobacka, A. Ivaska, A. Lewenstam; *Electroanalysis* **2003**, 15, 336.
[165] J. Bobacka, T. Lindfors, A. Lewenstam, A. Ivaska; *Am. Lab.* **2004**, 36, 13.
[166] J. Bobacka, T. Lindfors, M. McCarrick, A. Ivaska, A. Lewenstam; *Anal. Chem.* **1995**, 67, 3819.
[167] A. Michalska, K. Maksymiuk; *Anal. Chim. Acta* **2004**, 523, 97.
[168] X. Zhang, B. Ogorevc, J. Wang; *Anal. Chim. Acta* **2002**, 452, 1.
[169] E. Barsoukov, J.R. Macdonald; *Impedance Spectroscopy: Theory, Experiment and Applications*, Wiley-Interscience; 2nd ed., 2005.
[170] C. Gabrielli, in: I. Rubinstein (ed.) *Physical Electrochemistry: Principles, Methods and Applications,* Marcel Dekker, New York, 1995 (p. 243)
[171] M. Sluytersrehbach; *Pure and Appl. Chem.* **1994**, 66 1831.
[172] D.D. MacDonald; *Electrochim. Acta* **2006**, 51, 1376.
[173] E. Warburg; *Wied. Ann.* **1899**, 67, 493.
[174] E. Warburg; *Drud. Ann.* **1901**, 6, 125.
[175] F. Krüger; *Z. Phys. Chem.* **1903**, 45, 1.
[176] G. Jaffé; *Ann. Phys.* **1933**, 16, 217 and 249.
[177] B. Tribollet, J. Newman; *J. Electrochem. Soc.* **1984**, 131, 2780.
[178] C. Dan, B, Van den Bossche, L. Bortels, G. Nelissen, J. Deconinck; *J. Electroanal. Chem.* **2001**, 505, 12.

[179] J.R. Macdonald; *J. Chem. Phys.* **1973**, 58, 4982.
[180] J.R. Macdonald; *J. Chem. Phys.* **1974**, 61, 3977.
[181] C. Gabrielli, P. Hemery, P. Letellier, M. Masure, H. Perrot, M. Rahmi, M. Turmine; *J. Electroanal. Chem.* **2004**, 570, 275.
[182] T.M. Nahir, R.P. Buck; *Electrochim. Acta* **1993**, 570, 2691.
[183] B. Grysakowski, A. Lewenstam, M. Danielewski; *Diff. Fund.* **2008**, 8, 4.1.
[184] D. Calvo, J. Bartrolí, M. del Valle; *Electrochim. Acta,* **2006**, 51, 1569.
[185] D. Whitley, S. Rana, R.B. Hackendorn; *Island Model Genetic Algorithms and Linearly Separable Problems,* AISB 1997, Workshop on Evolutionary Computingm Manchester, 1997.
[186] E. Cantu-Paz; *Efficient and Accurate Parallel Genetic Algorithms*. Kluwer Academic Publishers, Norwell, MA, 2000.
[187] T. Burczyński, W. Beluch, A. Długosz, W. Kuś, M. Nowakowski, P. Orantek; *Computer Assisted Mechanics and Eng. Sci.* **2002**, 9, 1, 3.
[188] J. Kołodziej, R. Gwizdała, J. Wojtusiak; *Hierarchical Genetic Strategy as a Method of Improving Search Efficiency, Advances in Multi-Agent Systems*, Jagiellonian University Press, 2001. , p. 149.
[189] J. Kołodziej; *Modelling Hierarchical Genetic Strategy as a Family of Markov* Chains**,** R. Wyrzykowski et al. (Eds.): PPAM 2001, LNCS 2328, p. 595, 2002. Springer-Verlag Berlin Heidelberg 2002.
[190] A. Semczuk, B. Wierzba; *MSc. Thesis,* Jagiellonian University, Krakow 2003.
[191] J. Kołodziej, R. Schaefer, A. Paszyńska; *Journal of Theoretical and Applied Mechanics, Computational Inteligence* **2004**, 42, 519.
[192] B. Wierzba, M. Danielewski; *Stochastic searching of diffusivity in multicomponent alloys by hierarchical genetic strategy*; Vísnik Čerkas'kogo Uníversitetu. Seríâ: Fíziko-Matematiční Nauki.; **2008**, 141, 14.
[193] K. Holly, M. Danielewski; *Phys. Rev. B* **1994**, 50, 13336.
[194] O. Auciello, J. Engenmann; *Multicomponent and Multilayered Thin Films for Advanced Microtechnologies*: *Techniques, Fundamentals and Devices*; vol. 234, NATO ASI Series, 1989.
[195] M. Piecuch, L. Nevot; *Mater. Sci. Forum* **1990**, 93, 59.
[196] M.L. Yang, X.H. Zhang, X.H. Li, X.H. Wu; *J. Electroanal. Chem.* **2002**, 519, 1.
[197] O. Kanoun, U. Tröltzsch, H.-R. Tränkler; *Electrochim. Acta* **2006,** 51, 1453.
[198] E.D. Moorhead, G.M. Frame II; *J. Phys. Chem.* **1968**, 72, 3684.
[199] J.E.J. Schmitz, J.G.M. van der Linden; *Anal. Chem.* **1982**, 54 1879.
[200] H. Zhou, S. Dong; *J. Electroanal. Chem.* **1997**, 425, 55.
[201] M. Rosvall; *Electrochem. Comm.* **2000**, 2, 791.
[202] G.A. Rechnitz, G.C. Kugler; *Anal. Chem.* **1967**, 39, 1682.
[203] K. Tóth, I. Gavallér, E. Pungor; *Anal. Chim. Acta* **1971***,* 57, 131.
[204] B. Fleet, T.H. Ryan, M.J.D. Brand; *Anal. Chem.* **1974**, 46, 12.
[205] P.L. Markovic, J.O. Osburn; *AIChE J.* **1973**, 19, 504.
[206] E. Lindner, K. Tóth, E. Pungor; *Anal. Chem.* **1976**, 48, 1051.
[207] G.A. Rechnitz, H.F. Hameka; *Fresenius, Z. Anal. Chem.* **1965**, 214, 252.
[208] W.E. Morf, E. Lindner, W. Simon; *Anal. Chem.* **1975**, 47, 1596.
[209] E. Lindner, K. Tóth, E. Pungor; *Anal. Chem.* **1982**, 54, 72.
[210] M. Gratzl, E. Lindner, E. Pungor; *Anal. Chem.* **1985**, 57, 1506.
[211] A. Lewenstam, A. Hulanicki, T. Sokalski; *Anal. Chem.* **1987**, 59, 1539.
[212] B. Paczosa-Bator, T. Błaż, J. Migdalski, A. Lewenstam; *Bioelectrochemistry* **2007**, 71, 66.
[213] E. Bakker, P.Buhlmann, E. Pretsch; *Talanta* **2004**, 63, 3.
[214] M. Maj-Żurawska, A. Lewenstam; *Anal. Chim. Acta* **1990**, 236, 331.
[215] J. Migdalski, T. Błaż, B. Paczosa, A. Lewenstam; *Microchim. Acta* **2003**, 143, 177.
[216] B. Paczosa, T. Błaż, J. Migdalski, A. Lewenstam; *Pol. J. Chem.* **2004**, 78, 1543.
[217] B. Paczosa-Bator, J. Migdalski, A. Lewenstam; *Electrochim. Acta* **2006**, 51, 2173.
[218] D.S. Silvester, E. Grygolowicz-Pawlak, E. Bakker; *Electrochem. Comm.* **2010**, 12, 110.
[219] S. Lal, G.B. Christien; *Anal. Lett.* **1970**, 3, 11.
[220] S.M. Hammond, P.A. Lambert; *J. Electroanal. Chem.* **1974**, 53, 155.

[221] S. Srianujata, W.R. White, T. Higuchi, L.A. Sternson; A*na. Chem.* **1978**, 50, 232.
[222] W.E. Morf, G. Kahr, W. Simon; *Anal. Lett.* **1974**, 7, 9.
[223] A. Lewenstam, E. Erkola, A. Lehmenkühler; *Fresenius J. Anal. Chem.* **1993**, 346, 577.
[224] P. Mueller, D.O. Rudin, H. Ti Tien, W.C. Wescott; *Nature* **1967**, 194, 979.
[225] G. Eisenman; *Membranes* vol.2, Dekker, New York, 1973.
[226] P. Läuger, G. Stark; *Biochim. Biophys. Acta* **1970**, 211, 458.
[227] D.A. Haydon, S.B. Hladky; *Q. Rev. Biophys.* **1972**, 5, 187.
[228] S.B. Hladky; *Biochim. Biophys. Acta* **1974**, 352, 71.
[229] G. Eisenman, S. Krasne, S. Ciani; *Ann. N. Y. Acad. Sci.* **1975**, 264, 34.
[230] S. Ciani; *J. Membrane Biol.* **1976**, 30, 45.
[231] W.E. Morf, E. Pretsch, N.F de Rooij; *J. Electroanal Chem.* **2010**, 642, 45.
[232] K. Dołowy; private communication.
[233] G.J. Siegel, B.W. Agranoff, S.K. Fisher, R.W. Albers, M.D. Uhler, ed. (1999). *Basic Neurochemistry* (6 ed.). Lippincott Williams & Wilkins.
[234] J.M. Zytkow, A. Lewenstam; *Fresenius J. Anal. Chem.***1990**, 338, 225.

ISBN 978-952-12-2938-1